

**PREDICTION OF SELECTIVE NEUROPROTECTIVE JNK3 INHIBITORY ACTIVITY OF
PLUMBAGIN AND ITS DERIVATIVES USING *INSILICO* COMPUTATIONAL
METHODS**



**Dissertation submitted to
THE TAMILNADU Dr. M.G.R. MEDICAL UNIVERSITY,
Chennai-600 032**

**In partial fulfillment of the requirements for the award of the
Degree of**

**MASTER OF PHARMACY
IN
PHARMACOLOGY**

**Submitted by
SUSMITHA P
REGISTRATION NO: 261925909**

**Under the guidance of
Dr. M. Ramanathan, D.Sc.,
Department of Pharmacology**



**PSG COLLEGE OF PHARMACY
PEELAMEDU
COIMBATORE 641004**

OCTOBER 2021

Certificates



Dr. M. Ramanathan, D.Sc.,
Principal & Head of the Department,
Department of Pharmacology,
PSG College of Pharmacy,
Peelamedu,
Coimbatore- 641004. (T.N)

CERTIFICATE

This is to certify that the dissertation work entitled “**PREDICTION OF SELECTIVE NEUROPROTECTIVE JNK3 INHIBITORY ACTIVITY OF PLUMBAGIN AND ITS DERIVATIVES USING *INSILICO* COMPUTATIONAL METHODS**” submitted by **University Reg No.261925909** is a bonafide work carried out by the candidate under the guidance of **Dr. M. Ramanathan, D.Sc.,** Principal & Head, Department of Pharmacology, PSG College of Pharmacy and submitted to The Tamil Nadu Dr. M.G.R. Medical University, Chennai, in partial fulfillment for the Degree of **Master of Pharmacy in Pharmacology** at the Department of Pharmacology, PSG College of Pharmacy, Coimbatore, during the academic year 2020-2021.

Place: Coimbatore

Date:

Dr. M. RAMANATHAN, D.Sc.,

Guide / Principal.

DECLARATION

I do hereby declare that the dissertation work entitled “**PREDICTION OF SELECTIVE NEUROPROTECTIVE JNK3 INHIBITORY ACTIVITY OF PLUMBAGIN AND ITS DERIVATIVES USING *INSILICO* COMPUTATIONAL METHODS**” submitted to The Tamil Nadu Dr. M.G.R. Medical University, Chennai, in partial fulfillment for the Degree of **Master of Pharmacy in Pharmacology**, was done by myself under the guidance of **Dr. M. Ramanathan, D.Sc.**, Principal & Head, Department of Pharmacology, PSG College of Pharmacy, Coimbatore, during the academic year 2020-2021.

Reg.No.261925909

EVALUATION CERTIFICATE

This is to certify that the dissertation work entitled “**PREDICTION OF SELECTIVE NEUROPROTECTIVE JNK3 INHIBITORY ACTIVITY OF PLUMBAGIN AND ITS DERIVATIVES USING *INSILICO* COMPUTATIONAL METHODS**” submitted by University **Reg. No. 261925909** is a bonafide work carried out by the candidate under the guidance of **Dr. M.Ramanathan, D.Sc.**, and submitted to The Tamil Nadu Dr. M.G.R. Medical University, Chennai in partial fulfillment for the Degree of **Master of Pharmacy in Pharmacology**, PSG College of Pharmacy, Coimbatore and was evaluated by us during the academic year 2020-2021.

Examination Center: PSG College of Pharmacy, Coimbatore.

Date:

Internal Examiner

External Examiner

Acknowledgement

ACKNOWLEDGEMENT

Behind every achievement there are many helping hands that aid in reaching the ultimate goal.

*I consider it as a great honor to express my deepest sense of gratitude to my beloved guide, **Dr. M. Ramanathan, D.Sc.**, Principal & Head, Department of Pharmacology, PSG College of Pharmacy, who was guiding me at every stage of the project and for keeping me in high sprit. His innovative and constructive ideas have been very invaluable, which made the work interesting and easy.*

*I would like to extend my heartfelt thanks to **Dr. Karthik Dhananjayan, M.Pharm., Ph.D.**, **Dr. S. Muthukrishnan, M. Pharm, Ph.D.**, for their support during the whole period of study.*

*I would like to dedicate a special thanks to **Mr. Ram Pravin kumar M.Pharm** for their constructive and valuable ideas for the completion of my project.*

*I would like to specially thank my batchmates **Mr.Senthil kumar, Mr.Gurubarath**, their support throughout the course of study & my project mates **Mr.Naveen Raj, Ms.Dhanalakshmi***

*I also thank our technical assistants **Mr.Azad Kumar, Mrs.Chitra Priya, and Mrs. Ambika** for their support during my project.*

*I express my sincere thanks to my senior **Mr. Dhanapal , Research Scholar**, Department of Pharmacology, for his support during the study period.*

*I owe my most sincere gratitude to **PSG Sons and Charities** for providing all the facilities to carry out this work.*

I am thankful to all my friends, who directly or indirectly helped me during the work.

Dedicated to
My lovable parents,
Beloved teachers
Friends & God

Contents

LIST OF CONTENTS

S.NO	CONTEXT	PAGE NO.
1.	INTRODUCTION	1
2.	REVIEW OF LITERATURE	4
3.	AIM AND OBJECTIVE	22
4.	PLAN OF STUDY	23
5.	MATERIALS AND METHODS	24
6.	RESULTS	29
7	DISCUSSION	63
8	CONCLUSION	66
9	REFERENCES	67

LIST OF FIGURES

Figure. No	TITLE	Page No
1	JNK signaling pathway	4
2	The JNK signaling pathway in the mammalian brain.	5
3	Downstream signalling JNK pathway	6
4	JNK signaling in the pathogenesis of neurodegenerative diseases	11
5	Schematic representation of the mechanism of action of JNK inhibitors	12
6	Structure of Plumbagin	16
7	Structure activity relationship of Plumbagin	17
8	Summarization of molecular-biological effects of plumbagin	21
9	JNK3 protein validation-Alignment of redocked conformations.	29
10	A ribbon diagram of the JNK3 protein	30
11	Interaction of ATP and JNK3 inhibitors with 3OY1	32
12	The N-terminal domain, C-terminal domain and activation loop	32
13	Generated pharmacophore hypothesis for SP600125	43
14	Generated pharmacophore hypothesis for AS601245	43
15	Generated pharmacophore hypothesis for Transertib (CC-930)	44
16	2D and 3D interaction diagram of 5-Methoxy-2-methyl-3-(4-(trifluoromethyl)benzylamino) naphthalene 1,4-dione from SP600125 hypothesis	46
17	2D and 3D interaction diagram of Shikonin from AS6001245 and CC-930 hypothesis	46
18	2D and 3D interaction diagram of 3-(4-Fluorobenzylamino)-5-methoxy-2-methylnaphthalene-1,4-dione , from SP600125 hypothesis	46

19	2D and 3D interaction diagram of Plumbagin-5-o-glucoside, from AS6001245 and CC-930 hypothesis	47
20	2D and 3D interaction diagram of Chitranone from SP600125 hypothesis	47
21	2D and 3D interaction diagram of plumbagin from AS6001245 hypothesis	47
22	Overlay of 5-Methoxy-2-methyl-3-(4-(trifluoromethyl)benzylamino) naphthalene 1,4-dione with SP600125 hypothesis	49
23	Overlay of Shikonin with AS6001245 hypothesis	49
24	The RMSD plot obtained for protein-ligand complex	56
25	Histogram chart of JNK3 protein (PDB ID: 3OY1) with 5-Methoxy-2-methyl-3-(4(trifluoromethyl)benzylamino) naphthalene 1,4-dione	57
26	The 2D diagram interaction of ligand-protein contacts.	58
27	The RMSD plot obtained for protein-ligand complex (shikonin with Jnk3)	59
28	Histogram chart of JNK3 protein (PDB ID: 3OY1) with shikonin	60
29	The 2D diagram interaction of ligand-protein contacts. (shikonin with Jnk3)	61
30	Schematic illustration of the overall workflow	62

LIST OF TABLES

Table No	TITLE	Page No
1	Summary of G-score and common amino acid residues interaction in JNK3 protein	33
2	Phase database compounds of Plumbagin derivatives and its structure	35
3	Pharmacophore and glide docking results for best G-score compounds from hypothesis (SP600125, AS6001245, and CC-930)	48
4	Qikprop results for reference compounds and top five plumbagin derivatives	51
5	Lipinski properties of compounds using Qikprop	51
6	Prime MM-GBSA energy properties of selected compounds and corresponding reference compounds	53

Abbreviations

LIST OF ABBREVIATIONS

JNK	c-Jun N-terminal Kinase
MAPK	mitogen-activated protein kinase
SAP/JNK	stress stimulate the stress-activated protein kinase/c-Jun N-terminal kinase
PLB	Plumbagin
NF- κ B	Nuclear factor kappa B
PDB	Protein data bank
Nrf2/ARE	Nuclear factor-erythroid 2-relatedfactor-2 /antioxidant response element
H-bond	Hydrogen bond
G-Score	Glide score
ADME	Adsorption, Distribution, Metabolism and Excretion
MM/GBSA	Molecular mechanics- generalized born surface area
Rule of Five	Number of violations of Lipinski's rule of five
MW	Molecular Weight of the molecule
QPlogP o/w	Predicted octanol/water partition coefficient
QPlogBB	Predicted brain/blood partition coefficient
QPPCaco	Predicted Caco cell permeability
Q Plog HERG	Predicted IC50 value for blockage of HERG K ⁺ channels
Q Plog S	Predicted aqueous solubility in mol/L
PMDCK	Predicted apparent masindarby canine kidney cell permeability
MD	Molecular dynamics simulation
SPC	Simple point charge
RMSD	Root mean square deviation
RMSF	Root mean square fluctuations
PL contacts	Protein-Ligand contacts
LP contacts	Ligand-Protein contacts
XP	Extra precision
MET	Methionine
ILE	Isoleucine

ASN	Asparagine
GLY	Glycine
IC50	Half maximum concentrations
ALA	Alanine
VAL	Valine

Introduction

1. INTRODUCTION

Neurodegenerative diseases (NDs) represent a common neurological pathology that determines a progressive deterioration of the brain or the nervous system. Neurodegenerative Diseases (NDs) are defined as a fatal and debilitating condition resulting in the intensifying death of nerve cells. As members of the MAPK family, c-Jun-N-terminal kinases (JNKs) regulate the biological processes of apoptosis. In particular, the isoform JNK3 is expressed explicitly in the brain at high levels and is involved in the pathogenesis of neurodegenerative diseases such as Alzheimer's disease (AD) and Parkinson's disease (PD), Huntington's disease (HD), multiple sclerosis (MS), motor neuron disease (MND). The human brain is the most affected organ due to its sensitivity to the oxygen level in the blood and high oxygen demand. The kinase c-Jun N-terminal Kinase 3 (JNK3) plays an important role in neurodegenerative diseases.

c-Jun N-terminal Kinase (JNK) is a serine/threonine kinase that is one of the members of the mitogen-activated protein kinase (MAPK) family and it is activated by pro-inflammatory cytokines or exposure to environmental stress such as heat shock, ionizing radiation, growth factors and also from internal stressors such as oxidative stress and DNA damage, DNA and protein synthesis inhibition response to endoplasmic reticulum stress. JNK3 Serine/threonine-protein kinase involved in various processes such as neuronal proliferation, differentiation, migration and programmed cell death. Extracellular stimuli such as proinflammatory cytokines or physical stress stimulate the stress-activated protein kinase/c-Jun N-terminal kinase (SAP/JNK) signaling pathway. JNK3 mainly expressed in the CNS is the most sensitive isoform to stress stimulation, suggesting that it is an important target and biomarker for the treatment of neurodegenerative diseases. (Zhao et al., 2021)

The JNK pathway plays a major role in apoptosis. JNK is a multifunctional kinase involved in many physiological and pathological processes. JNK plays an important role in the brain ischemic and related damages. JNK pathway is generally a "death" signaling pathway. The normal JNK pathway is essential for neurodevelopment and neuronal regeneration. JNK pathway plays an important role in primary sensory neurons after tissue or nerve injury, JNK signaling pathway is associated with the pathogenesis of several diseases including diabetes, rheumatoid arthritis, inflammatory disorders, vascular diseases, cancer and neurological diseases. JNK can induce apoptosis in response to a variety of stresses. They differ in their tissue expression profile and functions, with JNK1 and JNK2 being widely expressed, whereas JNK3 highly expressed in the brain and most responsive to stress stimuli in CNS and lesser extent in cardiac smooth muscle and testis.

JNK3 Mostly involved in neurodegenerative disease like Alzheimer's disease, Parkinson's disease, cerebral ischemia and other CNS disorder. JNK3 plays key role in brain function under normal and pathological condition. JNK3 has been implicated in brain development, neurite formation, plasticity in addition to memory and learning. JNK3 is involved in several neurodegenerative diseases both acute and chronic. JNK3 activation has a important role in triggering apoptosis and neuronal death. JNK3 activation is pro-apoptotic pathway in hippocampus neurons. consistent with a role for JNK3 in excitotoxic neuronal cell death. JNK3 has been identified as a promising target for potential treatment of neurodegenerative disorders .Aminopyrazoles, amino pyridines, aminopyrimidines, indazoles, pyridine Carboxamide, are some molecule already reported as ATP competitive JNK inhibitors. **(Qinghua Wua et al., 2020)** suggested that JNK3 is the major kinase for APP phosphorylation at T668. Similar mechanism of action to SP600125, AS601245 blocks JNK3 with a greater potency than JNK1 and JNK2.

Many medicinal plants such as, *Lyciumbarbarum*, *Melissa officinalis*, *Momordicacharantia*, *Cyperusrotundus* etc. possessed neuroprotective effect by many mechanisms. Natural antioxidants such as polyphenols, curcumin, resverastrol, and xanthone have been shown to possess neuroprotective activity in experimental models. Further, the research towards finding effective neuroprotective agent from natural origin is the current theme of our study. Phytochemicals from medicinal plants play a vital role in maintaining the brain's chemical balance by influencing the function of receptors for the major inhibitory neurotransmitter **(Kumar et al., 2012)**. Phytochemicals protect neuron by targeting multiple pathogenic factors of neurodegenerative disorders. Phytochemicals, importantly those having electrophilic structure have recently increased attention because their ability to induce cell survival responses like detoxification and antioxidant effects.

Plumbagin is a phytochemical (5-hydroxy-2-methyl-1, 4-naphthoquinone) which is naturally accuringnaphthoquinone isolated from the roots of medicinal plant of plumbago genus, *plumbago indica*, *Plumbagozeylanica*, *Plumbagorosea*, and *Plumbagoauriculata*, belonging to the family Plumbaginacea. In some studies shows that plumbagin have neuroprotection by Nrf2-ARE pathway and also have variety of uses like potential anti-inflammatory, antioxidant, anti-proliferative, anti-atherosclerotic, anticoagulant, anti-fertility, antifungal, anti bacterial, anti-angiogenic, anticancer etc.**(Jangra et al., 2021)** . PLB, a natural compound, has shown potent anti-proliferative effects by regulating various signaling pathways related to cell cycle and apoptosis. Plumbagin produced anti-inflammatory effect by suppressing the activation of nuclear factor kappa B (NF-κB). Plumbagin

protects against cerebral ischemia and spinal cord injury-induced oxidative stress and inflammation by activating the nuclear factor-erythroid 2-related factor-2 /antioxidant response element (Nrf2/ARE) pathway. Plumbagin has shown to promote generation of astrocytes and neuronal cell proliferation. Plumbagin showed potent anti-inflammatory effect by inhibiting the expression of COX-2 without affecting COX-1 (**Luo et al., 2010**). Among botanical pesticides, especially plumbagin have reported neuroprotective properties and it also promotes the generation of astrocytes from rat spinal cord neural progenitors via transcription factor activator.

In silico approaches provide an alternative method with low cost that has been successfully implemented to cure ND disorders in recent days (**Rai et al., 2020**).

- In this study, selective neuroprotective JNK3 inhibitory activity of plumbagin and its derivatives will be predicted by using *in silico* computational methods.
- An energetically minimized structure-based pharmacophore hypothesis for JNK3 inhibitors will be developed.
- Molecular docking studies will be conducted for plumbagin and its derivatives with crystal structure of JNK3 inhibitor to determine binding affinity.
- Qikprop module will be used to analyze ADME (Adsorption, Distribution, Metabolism and Excretion) druglikeness, toxicity profile.
- The binding free energy of most promising compounds will be estimated by using MM/GBSA.
- The stability of the docked Protein-ligand complex will be evaluated via Molecular dynamics by using of Schrödinger V7.7.

Review of literature

2. REVIEW OF LITERATURE

2.1 JNK signaling pathway

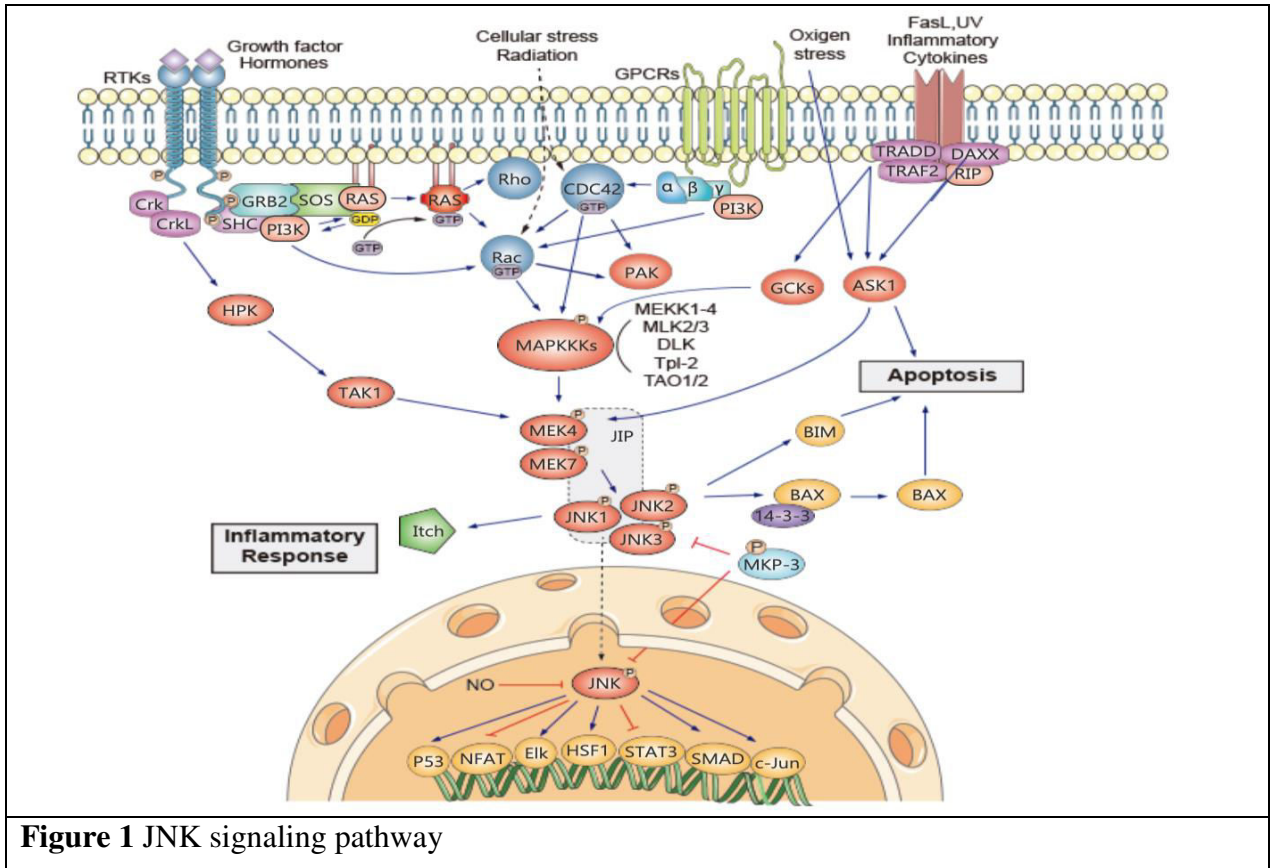


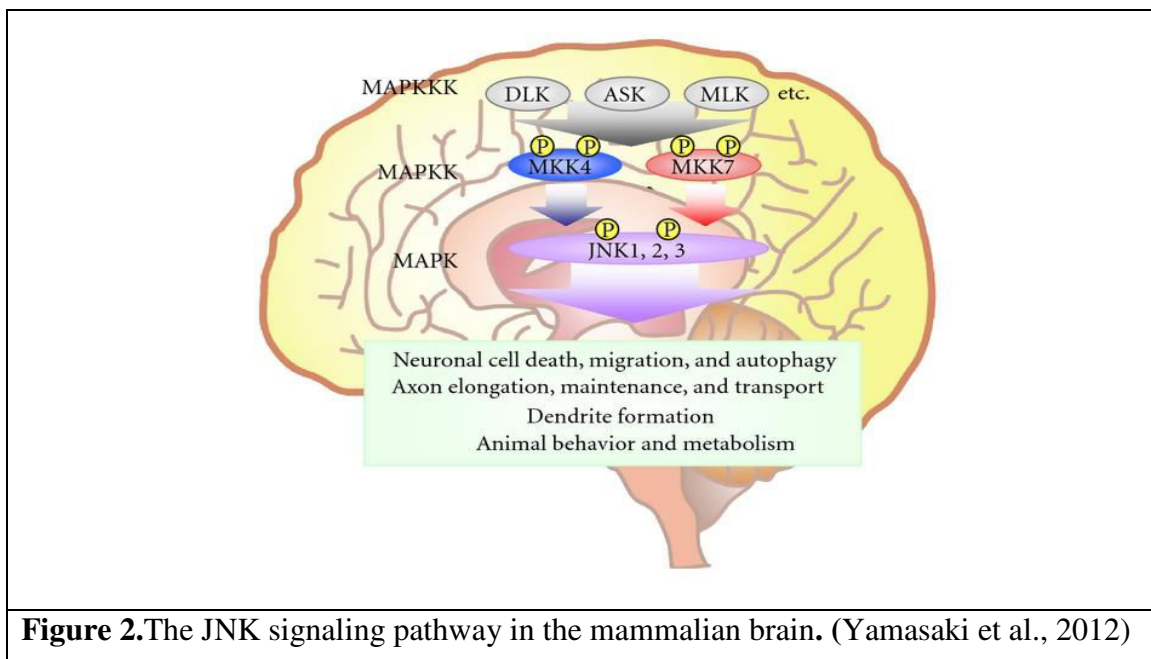
Figure 1 JNK signaling pathway

2.1.1 JNK signaling

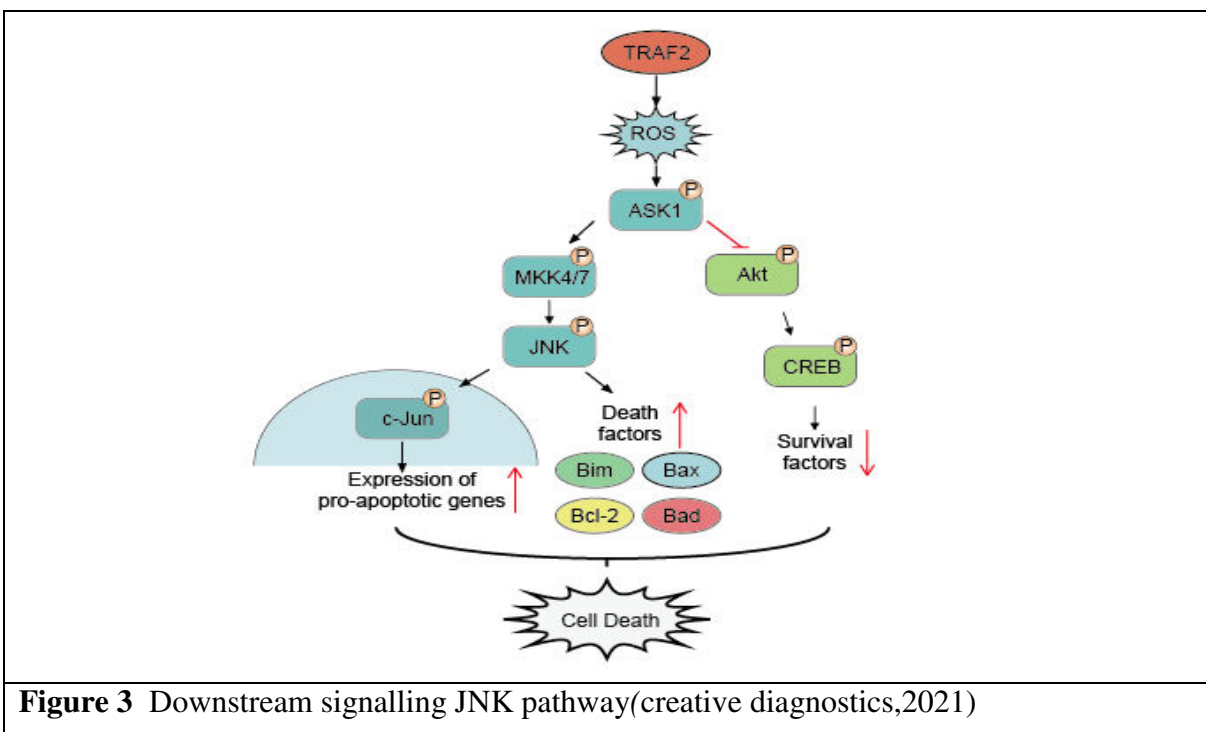
JNK, a member of the mitogen- activated protein kinase family, plays an important role in apoptosis. JNK pathway is generally a “death” signaling pathway. JNKs are encoded by three genes: *jnk1* (MAPK8), *jnk2* (MAPK9), and *jnk3* (MAPK10). JNK1 and JNK2 are expressed in most tissues, while JNK3 is selectively expressed in the brain, heart, and testis. The JNK module plays an important role in apoptosis, inflammation, cytokine production, and metabolism. C-jun n-terminal kinase is activated by environmental stress (ionizing radiation, heat, oxidative stress, and DNA damage and inflammatory cytokines, NGF, β -amyloid exposure, TNF, UV irradiation, Low potassium excitotoxic stress (Yarza et al., 2016). JNK pathway is activated through G protein-coupled receptors (GPCRs) using such as G12/13. Initiated by mitochondrial events

(Dhanasekaran et al., 2008). JNK3 kinase plays a critical role in neurotoxicity. It has also been implicated in the progression of many life-threatening neuronal and metabolic disorders (Braithwaite et al., 2010). JNK is a prominent mediator of pathological events and is associated with neuroinflammation and neurodegeneration.

MKK7 also called stress-activated protein kinase/extracellular signal regulated protein kinase kinase-2. The loss of MKK7 leads to decreased proliferation. MKK4 is strongly activated by environmental stress, while MKK7 is activated by both inflammatory cytokines and environmental stress. Recent studies indicate that although MKK4 and MKK7 phosphorylate JNK on both Thr and Tyr residues. MKK4 preferentially phosphorylates JNK on Tyr and MKK7 preferentially targets on Thr (Tournier et al., 2018). MKK4 and MKK7 activation is in turn mediated by various MAPKKKs (e.g., apoptosis signal-regulating kinases, ASKs; mixed lineage protein kinases, MLKs; and dual leucine zipper kinase, DLK); moreover the JNK signaling pathway is also modulated by different scaffold proteins, as the JNK-interacting protein (JIP)1, JIP2, and JIP3 (Dickens et al., 1997) (Yasuda et al., 1999)



JNK signaling pathway is such a death pathway that control cell death. There are two main downstream signaling of JNK pathway: one is activation of death signaling such c-Jun, Fos and apoptosis signaling such as BIM, BAD, BAX protein or active P53 transcription, to promote cell apoptosis; the other is inhibition of the cell survival signaling such as STATs and CREB



2.1.2 Mechanism:

- JNK can promote apoptosis by two distinct mechanisms. In the first mechanism targeted at the nuclear events, activated JNK translocates to the nucleus and transactivates c-Jun and other target transcription factors (TF). JNK can promote apoptosis by increasing the expression of pro-apoptotic genes through the transactivation of c-Jun/AP1-dependent or p53/73 protein-dependent mechanisms.
- JNK phosphorylates the BH3-only family of Bcl2 proteins to suppress the anti-apoptotic activity of Bcl2 or Bcl-XL.
- JNK can stimulate the release of cytochrome c (Cyt C) from the mitochondrial inner membrane through a Bid-Bax-dependent mechanism, promoting the formation of apoptosomes consisting of cytochrome c, caspase-9 (Casp 9) and

Apaf-1. This complex initiates the activation of caspase-9-dependent caspase cascade.

- JNK promotes apoptosis by inhibiting the antiapoptotic proteins such as Bcl2. JNK can also phosphorylate several other transcription factors including JunD, ATF2, ATF3, Elk-1, Elk-3, p53, RXRa, RARb, AR, NFAT4, HSF-1 and c-Myc (Johnson et al., 2007)

2.1.3 JNK in nervous system disease:

JNK3 activation is a pro-apoptotic pathway in hippocampus neurons consistent with a role for JNK3 in excitotoxic neuronal cell death. The role of JNK3 in excitotoxicity suggested that JNK/ SAPK pathways would be involved in other neuronal death responses and neurodegenerative diseases. A clear role of JNK/ SAPKs in ischemia-induced cell death has been demonstrated in mice. JNK3 may also prove to be a therapeutic target for neurodegenerative diseases including Parkinson's and Alzheimer's disease. JNK3 directly phosphorylates Tau proteins facilitating the formation of neurofibrillary tangles, positive correlated with cognitive impairment and neuronal loss.

JNK/SAPKs are clearly involved in ischemia-induced cell death and reperfusion injury in several different tissues and the control of insulin sensitivity in metabolic regulation. There are many other suggestions in the literature that link JNK/SAPK signaling to additional human diseases such as type I diabetes, osteosarcoma, ataxia and immune system dysfunction. JNKs probably play a role in chronic inflammation, airway hyper responsiveness and protease-directed tissue remodeling. It may also be useful to develop specific MKKK inhibitors to selectively block JNK activation in response to different upstream inputs. (Jing et al., 2005)

2.1.4 Role of different JNKs

Hyperactivation of JNK signalling is a very common finding in a number of disease states including cancer, inflammatory and neurodegenerative disease. (Zhao et al., 2021) suggested that in the developing brain, JNK1 affects the morphology of dendrites by phosphorylating cytoskeleton regulatory proteins and participates in hippocampal long-term depression (LTD), while JNK2 plays an important role in long-term potentiation (LTP). JNK3 is the major isoform of stress stimulus activation and is mainly involved in the process of

neurodegeneration. JNK1 phosphorylates IRS-1, and JNK1 knockout mice are resistant to diet-induced obesity (Sabio et al., 2010). JNK2, often in concert with JNK1, has been implicated in the pathology of autoimmune disorders such as rheumatoid arthritis (Han et al., 2002) and asthma (Chialda et al., 2005). A recent study suggested that JNK2 may also play a role in vascular disease and atherosclerosis. However, to date, no inhibitors of JNK have been approved for use in humans.

Recent studies suggested that JNK1 and JNK2 play an important role in the development of diabetes, obesity, arthritis, cancer, and heart disease. JNK1 seems to be involved in the development of obesity-induced insulin resistance, which implies inhibition of JNK1 might be an effective way of treating type-2 diabetes. JNK3 has been shown to play important roles in the brain to mediate neurodegeneration, such as beta-amyloid processing, Tau phosphorylation and neuronal apoptosis in Alzheimer's disease, as well as the mediation of neurotoxicity in a rodent model of Parkinson's disease (Musi et al., 2020). JNK3 modifies the amyloid precursor protein (APP), which results in a stimulation of amyloid- β 42 (A β 42) peptide production. (O'Brien et al., 2011)

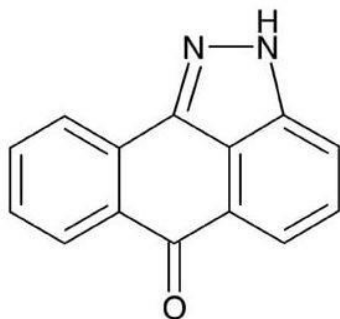
2.1.5 Structure and functions of JNK3

JNK3 is a protein kinase of the MAPK family that is Brain-selective JNK isoform. JNK3 is a multifunctional enzyme important in controlling brain functions under both normal and pathological conditions. JNK3 has been implicated in brain development, neurite formation and plasticity (Leach et al., 2015) in addition to memory and learning.

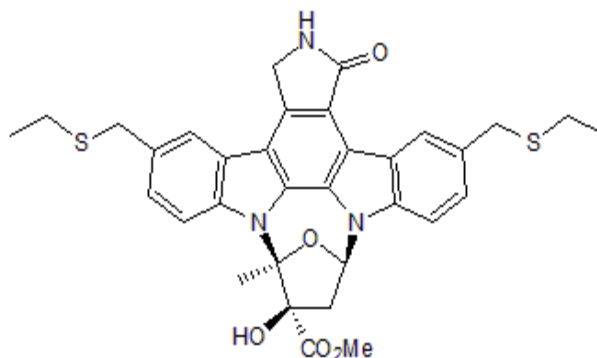
X-ray structure shows all JNK3 has two different lobes, N-terminal and C-terminal lobes. The N-terminal domain (residues 45-149 and 379-400) of JNK3 contains mostly β strands, whereas the C-terminal domain (residues 150-211 and 217-374) is predominantly α helical. A deep cleft between the two domains comprises the ATP-binding site, where the glycine-rich sequence (Gly71-Ser-Gly-Ala-Gln-Gly-Ile-Val78) of JNK3 forms a well-defined. The region spanning residues Ser217-Thr226 contains the JNK3 regulatory phosphorylation sites, Thr221 and Tyr223, and is referred to as the 'phosphorylation lip' or 'activation loop', have small segment commonly known as hinge region composed of five amino acid residues (Glu147-Leu148-Met149-Asp150-Ala151) in JNK3.

2.1.6 Neuroprotective effects of JNK inhibitors:

Activation of JNK has been identified as a key element responsible for the regulation of apoptosis signals. c-JNK pathway activation may be common step in various neurodegenerative diseases. The pharmacological inhibition of JNK is a suitable strategy to protect against neuronal death.



SP600125



CEP-1347

Several kinds of inhibitors have been developed, targeting different levels of the JNK signaling cascade and some of them, such as CEP-1347 and SP600125, have been used in clinical trials. SP600125 and AS601245, both selective inhibitors of JNK pathway. Intraperitoneal injection of SP600125 was effective in the MPTP mouse model of PD. AS601245 also displayed anti-inflammatory activity in an experimental model of rheumatoid arthritis. CEP-1347 is a small-molecule inhibitor of mixed lineage kinases (MLKs) and also enhances neuronal survival in a variety of nonclinical model (Davies et al., 2012).

(Wang et al., 2019) Reported that dopaminergic neurons were protected from apoptosis due to the inhibition of JNK by its specific inhibitor, SP600125. (Lange et al., 2015) exploited the sulfur atom of the gatekeeper residue Met146 for attractive hydrogen bonding interaction in the design of JNK3 aminopyrimidine-based inhibitors. A recent study shows that neuronal apoptosis induced by brain ischemia partly depends on the phosphorylation of JNK3. Activated JNK, in turn, phosphorylates c-Jun and those proteins associated with apoptosis such as Bcl-2 and P53

(Darusman et al., 2021) Revealed that Christinin compound molecules has potential to be developed as c-Jun N-terminal kinase (JNK) inhibitors candidate to control of skin infections

caused by *Propionibacterium acnes* which has potential as a topical anti-acne. The chitin molecules form a stable molecular interaction with the active binding site of the c-Jun N-terminal kinase (JNK) macromolecules.

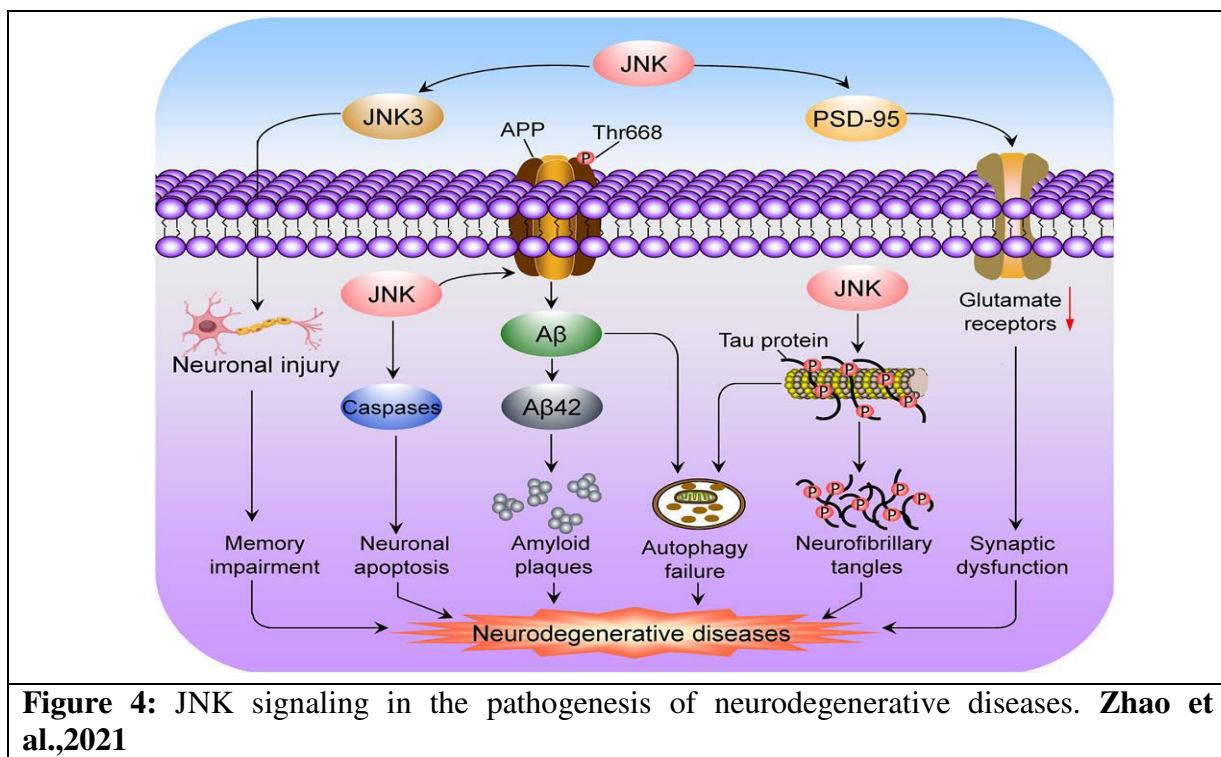
(Shen et al., 2021) Reported that Photobiomodulation inhibited JNK3 activity via the ERK/MKP7 pathway. JNK3 activity is decreased in APP/PS1 transgenic mice via PBM (635 nm, 6 J/cm², daily for 30 days), resulting in a dramatic reduction in amyloid load, AMPA receptor endocytosis, and inflammatory responses, thereby rescuing memory deficits. These studies suggested that PBM results in A β reduction by inhibiting the amyloidogenic pathway and is a promising therapeutic strategy via inhibiting JNK3.

(Syaifie et al., 2021) Suggested that Neurodegeneration occurs when nerve cells in the brain or peripheral nervous system lose function over time and eventually die. It is caused by an extracellular neurotoxic micro-environment associated with oxidative stress, chronic inflammation, and mitochondrial dysfunction. Dietary phytochemical supplementation is proving to be a promising nutritional intervention approach due to its neuroprotective properties as an antioxidant and anti-inflammation. Molecular docking is the preliminary study in drug design tools as a combination of computational techniques and biological molecular structure data to predict the interaction between the ligand and its protein target. propolis significantly inhibited the expression of pro-inflammatory cytokines such as IL-1 β , TNF- α , and IL-6, generation of ROS from mitochondria, and NF-KB activation.

(Huang et al., 2021) Reported that Zoledronic acid inhibits osteoclastogenesis and bone resorptive function by suppressing RANKL-mediated NF- κ B and JNK and their downstream signalling pathways. Zoledronic acid (ZOL) plays a pivotal role in regulating bone mineral density. ZOL also suppressed the activation of NF- κ B and the phosphorylation of c-Jun N-terminal kinase.

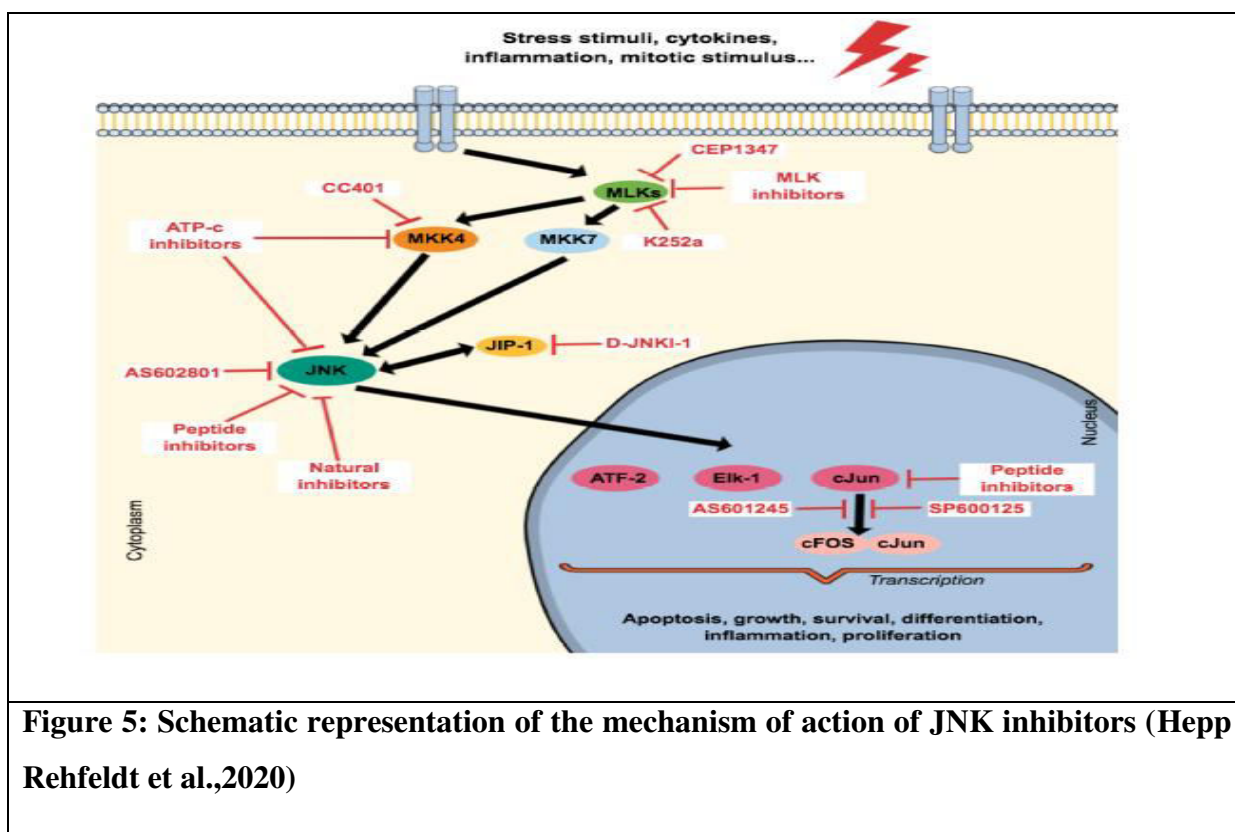
(Zhao et al., 2021) Described that c-Jun N-terminal kinase (JNK) signaling pathway is a potential therapeutic target for neurodegenerative diseases. Therefore JNK is involved in cell

proliferation, cytoskeleton construction, and cell malignancy.³ In particular, activation of JNK leads to synaptic dysfunction and even neuronal apoptosis, ultimately resulting in memory deficits and neurodegeneration. JNK phosphorylates the amyloid precursor protein and tau, ultimately resulting in the formation of extraneuronal senile plaques and intraneuronal neurofibrillary tangles. JNK3 is widely acknowledged, as a potential therapeutic target for CNS diseases.



(Joon-Hong, et al., 2021) Three pan-JNK inhibitors, SP600125, AS-602801, and Tanzisertib have been introduced and suggested to target JNK3 in neurodegenerative disease. SP600125 was the first reported potent pan-JNK inhibitor with poor selectivity over other MAPKs, such as p38 and Erk. Studies have showed that SP600125 leads to decreased formation of neurofibrillary tangles and oligomeric amyloid β plaques and improves AD-associated cognitive declines in APP^{swe}/PS 1dE9 double transgenic mice. AS602801 was another pan-JNK inhibitor identified in the process of drug development, but for other diseases. In 2012, AS602801 reached phase 2 clinical trial studies to evaluate its ability to treat inflammatory endometriosis. Tanzisertib, another potent pan-JNK inhibitor, was investigated for treatment of discoid lupus erythematosus in clinical trials in 2011.

(Qinghua, et al., 2020) JNK signaling is apparently involved in cancer development and progression. Therefore, JNK is an attractive target for therapeutic intervention with small molecule kinase inhibitors. Actually some ATP-competitive (e.g. SP600125) and ATP-non-competitive inhibitors have been developed; however, some limitations are noted in these inhibitors. For example, cell toxicity and a lack of specificity are observed due to their indiscriminate inhibition of the phosphorylation of all JNK substrates. During the last decade, some JNK inhibitors have been tested in many clinical trials. CC-401 is a second generation of ATP competitive inhibitors, shows antineoplastic activity. This compound shows a high capacity in the inhibition of JNK and is also seen to show efficacy in renal injury models. However, a phase I clinical trial using CC-401 for acute myeloid leukaemia was discontinued. Some inhibitors of JNK have been tested in the clinical study. PGL5001 (AS601245) is another ATP-competitive inhibitor and is currently being evaluated in a Phase II clinical trial.



(Singh et al., 2020) Investigated that the *insilico* docking studies against JNK protein to assess the anti-convulsant activity of synthesized hydrazone derivatives. Recently hydrazone derivatives have great importance due to their various biological properties and have multiple beneficial effects include anti-inflammatory, anticonvulsant, anticancer, antibacterial. Epilepsy is a chronic neurological disorder. JNK hyper-activation significantly correlated with pathogenesis of chronic epilepsy. JNK phosphorylation as a potential antiepileptic target in temporal lobe epilepsy. In this paper conduct *Insilico* docking studies of newly synthesized hydrazones derivatives against JNK protein and calculate binding affinities. In this research work 2-(3,4-dichloro-benzyl)-benzoic acid (4-fluoro-benzylidene)-hydrazide has high binding affinity for JNK3 protein (G-score -9.5kcal/mol) interaction with MET,SER,LYS. The Potential lead compound decreased the hyperactive of JNK signaling pathway and offered to treat epileptic patients.

(Youri, et al., 2020) Reported that 3-alkyl-5-aryl-1-pyrimidinyl-1H-pyrazole derivatives had highly selective JNK3 inhibitors with reduced molecular weights for better Brain-Blood Barrier permeability. Among the derivatives, the IC₅₀ value of **8a**, (R)-2-(1-(2-((1-(cyclopropanecarbonyl) pyrrolidin-3-yl) amino) pyrimidin-4-yl)-5-(3,4-dichlorophenyl)-1H-pyrazol-3-yl)acetonitrile exhibited 227 nM, showing the highest inhibitory activity against JNK3

(Jang et al., 2020) Reported that 1-pyrimidinyl-2-aryl-4,6-dihydropyrrolo[3,4-d]imidazole-5(1H)-carboxamide derivatives will be highly useful in the development of JNK3-selective inhibitors as therapeutic agents for neurodegenerative diseases. Sixteen compounds were synthesized and measured for their enzyme activity against JNK3. compound 18a, (R)-1-(2-((1-(cyclopropanecarbonyl)pyrrolidin-3-yl)amino)pyrimidin-4-yl)-2-(3,4-dichlorophenyl)-4,6-dihydro pyrrolo [3,4-d]imidazole-5(1H)-carboxamide, showed the highest IC₅₀ value of 2.69 nM. Kinase profiling results also showed high selectivity for JNK3 among 38 kinases, having mild activity against JNK2, RIPK3, and GSK3 β , which also involve in neuronal apoptosis.

(Zulfiqar et al., 2020) Reported that FDA-approved drugs dabigatran, estazolam, and pitavastatin demonstrated a superior affinity for JNK3, which was similar to the reference drug SP600125, as indicated by docking simulations. These drugs decreases the expressive of TNF- α ,

NF- κ B in cortex, striatum and H-bond interaction with Met 149, Met129, Lys 93. JNK involved not only in apoptotic pathway also in cell regulating mechanism such as cell proliferation, gene expression.

(Abdellahet et al., 2020) Reported that a series of tetra-substituted pyridinylimidazoles derivatives as JNK3 inhibitors were analyzed by using computer-aided drug design processes, such as 2D/3D-QSAR and molecular docking.

(Plotnikov et al., 2020) Suggested that 11H-indeno[1,2-b]quinoxalin-11-one oxime sodium salt (IQ-1S) inhibits JNK enzymatic activity in the hippocampus and protects against stroke injury when administered in the therapeutic and prophylactic regimen in the rat model of FCI and also has a high affinity to JNK3 compared to JNK1/JNK2.

(Chen et al., 2018) Described that JNK3 is one of the major MAPK family members in the brain. It is reported that calcium overload and oxygen free radicals can activate JNK3, thereby inducing the expression of apoptotic proteins such as p53 and FasL and inducing the expression of caspases, so as to accelerate the process of cell apoptosis. Therefore, this study aimed to investigate the effect of PI3K/Akt/mTOR signaling pathway on the expression of JNK3 in PD mice. Inhibition of PI3K/Akt/mTOR signaling pathway is negatively correlated with the expression of JNK3. Inhibition of PI3K-Akt-mTOR signaling pathway leads to a decrease in the expression of JNK3, which protects dopaminergic neurons and improves PD.

(Brandalise et al., 2017) Revealed that *Hericium erinaceus* bioactive compounds enhance the NGF mRNA expression in the hippocampus through the c-jun N-terminal kinase (JNK) pathway. In the AD mouse model, HE improves the spatial short-term and visual recognition memory by boosting hippocampal neurons.

(Jung et al., 2017) Found out a novel scaffold for JNK3 inhibitors and they performed 3D-QSAR studies include COMFA and COMSIA to explain activities of two different types of JNK inhibitor series such as 2-amino phenyl acetamide derivatives and N-(thiophen-2-yl) acetamide derivatives. Activation of JNK3 through phosphorylation leads to caspase activation, neuronal inflammation, A β aggregation, and apoptosis. JNK3 is major protein kinase for APP phosphorylation and important mechanism for A β processing. Targeting JNK3 is a reasonable strategy for drug discovery in ND. Based on 3D-QSAR such as COMFA and COMSIA models

successfully suggested N-(thiophen-2-yl)-8H-Pyrazolo [1,5-a] pyrido[1,2-c] pyrimidine-10-carboxamide as a novel scaffold for JNK3 inhibitor.

(Xiang-Ru wen et al., 2016) Reported that sevoflurane could suppress ischemic brain injury by downregulating the activation of the ASK1/JNK3 cascade via increasing the phosphorylation of Akt1 during ischemia/reperfusion. The activated ASK1/JNK3 signaling cascade mediates apoptosis, causing neuronal damage

(Yarza et al., 2016) JNK3 is a multifunctional enzyme important in controlling brain functions under both normal and pathological conditions. JNK3 has been implicated in brain development, neurite formation and plasticity **(Eminel et al., 2008)** in addition to memory and learning. Under pathological conditions, JNK3 has been considered as a degenerative signal transducer and it seems to be the isoform involved in over-activation of JNK after deleterious stress-stimuli in adult brain (ischemia, hypoxia, epilepsies). This principle is supported by the data on the reduced apoptosis of hippocampal neurons and reduced seizures induced by kainic acid in JNK3 knockout (-/-) mice, and by the notion that JNK3-/- mice are also protected against ischemia.

(Jang et al., 2013) Reported that JNK3 is involved in nerve cell apoptosis, neurological function recovery and neuronal regeneration. Down regulation of JNK3 expression in the peripheral area of the injured cerebral cortex in the early stages of traumatic brain injury may be associated with apoptosis of nerve cell. **(Long et al., 2013)** JNK3 involved in nerve cell apoptosis and neurofunctional recovery after traumatic brain injury. Activation of JNK3 could promote apoptosis of glial cells in spinal cord injury. The role of JNK3 in apoptosis was also established using JNK3-/- mice **(Mehan et al., 2011)**. JNK protein control neuronal polarity, axon growth/path finding and programmed cell death. Recent studies show that role for JNK in motor neuron diseases such amyotrophic lateral sclerosis and spinal muscular atrophy.

(Chen et al., 2018) Several reports have demonstrated that active JNK is involved in the phosphorylation of tau proteins including in stroke and traumatic brain injury. **(Ploia et al., 2011)** Furthermore, JNK3 knockout mice are remarkably resistant to kainic acid-induced excitotoxicity and attenuated neuronal death in the global ischemia-hypoxia model. Knocking out of the JNK3 gene condenses the apoptotic Bim and Fas activity after stroke and with parallel less cytochrome c release following oxygen-glucose deprivation. **(Morel et al., 2010)**

2.2 Plumbagin:

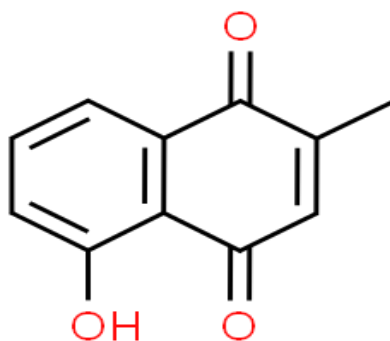


Figure: 6 Structure of Plumbagin: PubChem ID: 10205

Plumbagin is a hydroxy-1, 4-naphthoquinone that is 1,4-naphthoquinone in which the hydrogen at positions 2 and 5 are substituted by methyl and hydroxyl groups, respectively. Phytochemicals, importantly those having electrophilic structure have recently increased attention because their ability to induce cell survival responses like detoxification and antioxidant effects.

Plumbagin is a yellow dye, formally derived from naphthoquinone. Plumbagin phytochemical named (5-hydroxy-2-methyl-1,4-naphthoquinone. Plumbagin is a naphthoquinone which is mostly present in *Plumbago* species, which shows several pharmacological activities, including anti-inflammatory, neuroprotection (Yuan et al., 2017) antitumor activity and antioxidant effects, anti-fertility, antibacterial, and antifungal. Which is one of the simplest plant secondary metabolites of three major phylogenetic families viz. Plumbaginaceae, Droseraceae and Ebenaceae (Hazra et al., 2004). Plumbagin can produce different biological action in different cell type's i.e. in cancer cells PLA induces cell cycle arrest and apoptosis. (Wang et al., 2008) reported that Plumbagin induces cell cycle arrest and apoptosis through reactive oxygen species/c-Jun N-terminal kinase pathways in human melanoma A375. S2 cells. It also promotes generation of astrocytes from rat spinal cord neural progenitors via transcription factor activation. Botanical pesticides generally having a toxic property in higher doses so they usually studied for cancer therapeutic potentials.

Plumbagin was shown to induce apoptosis in both mouse and human T-cell lymphoma cell lines via increased oxidative stress, caspase activity and loss of mitochondrial membrane

potential, induction of cytochrome-c release, FasL expression, and high Bax levels via activation of the JNK pathway (Checker et al., 2018) In many signaling pathways, the key regulatory genes regulated by plumbagin are NF- κ B, STAT3, and AKT, etc. Plumbagin is also a potent inducer of ROS, suppressor of cellular glutathione, and causes DNA strand break by oxidative DNA base damages.

(Rajalakshmi et al., 2018) The 5th position hydroxyl group of PLB increases its electrophilic properties and makes it a more potent cytotoxic molecule via its ability to accept electrons which increases its capacity to generate ROS. In third position Substitution of N-acetyl-1-amino acid side chain its significantly increased antifeedant activity. Halogen substitution at third position it shown stronger ichthyotoxicity than free PLB. PLB homologues (2-alkyl-1,4-naphthoquinones) as well as their 3-methyl derivatives were shown weaker prostaglandin synthetase (PGS)-inhibition activity. Thioglycosides and alkylglucoside derivatives showed antibacterial activity by inhibiting N-acetylglucosaminyltransferase (MshB) and mycothiol-S-conjugate amidase (Mca) which are needed for mycothiol synthesis in bacteria. The PLB bind at C-3 position via 2–5 methylene carbons and an amide linkage to phenyl-2-deoxy-2-amino-1-thio- α -D-glucopyranoside was shown potent inhibitor of MshB. MshB inhibitory activity was shown by large carbon chain length substituted in PLB.

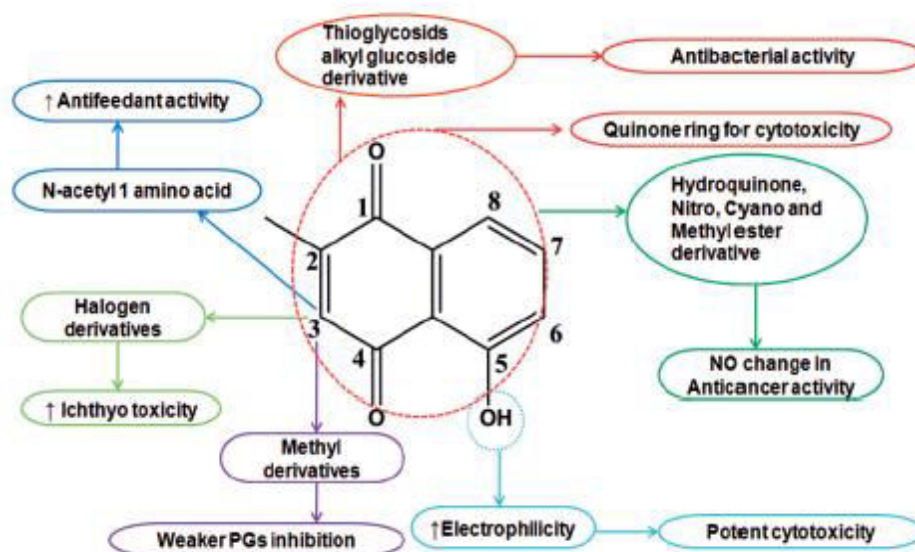


Figure 7: structure activity relationship of plumbagin

(**Banasri et al., 2002**) reported that cytotoxicity of compounds containing quinines structure might be due to radical formation via electron transport in the existence of quinone ring. Therefore, cytotoxicity of PLB may be associated with its special structure which contains a quinone ring. The hydroquinonoid, nitro, cyano and methyl ester derivatives of PLB did not show any marked enhancement in the tumour-inhibitory activity.

(**Nadhan et al., 2021**) Suggested that the roots of *Plumbago rosea* Linn. are the richest source of plumbagin. PLB Chemically identified as a naphthoquinone. Plumbagin (5-hydroxy-2-methyl-1,4-naphthoquinone) is a yellow crystalline substance present in the roots of *P. zeylanica*, *P. rosea*, *P. capensis* (syn. *P. auriculata* Thunb.), and *P. europea*, belonging to the family Plumbaginaceae. Plumbagin contains a 2-methyl-1,4-naphthoquinone skeleton (i.e., an aromatic methyl p-quinone moiety). The compound is steam volatile and sublimes at 90°C. (*P. rosea* L. and *P. zeylanica* L.) Is a very potent herbal drug and has well-proven hepatoprotective activity. (**Akhilraj et al., 2021**)

(**Zhang et al., 2021**) Reported that Plumbagin is a potential natural product which showed inhibitory effect on the growth of Ishikawa cells. PLB could activate the apoptotic pathway of death receptor. Plumbagin induced autophagy and apoptosis through PI3K/AKT signaling pathway, blocked the cell cycle of Ishikawa cells in G2/M phase, promoted apoptosis through death receptor and mitochondrial pathways, and blocked PI3K/AKT pathway to prevent cell invasion.

(**Shi et al., 2021**) Revealed that Plumbagin has a pleiotropic effect on various cellular functions. Some studies have reported that PLB displays anti-fibrotic properties in the lung, kidney and liver. PLB regulated tissue repair and collagen deposition in Traumatic tracheal stenosis rats. PLB regulates lung fibroblast activity and attenuates Traumatic tracheal stenosis in rats by inhibiting TGF- β 1/Smad and Akt/mTOR signaling pathways.

(**Xue et al., 2021**) Suggested that phytochemicals has been showed as outstanding resource for the treatment of various malignancies. Plumbagin (5-hydroxy-2-methyl-1, 4-naphthoquinone) is a naphthoquinone-derived yellow crystalline phytochemical, which has been showed to have anti-proliferative, pro-apoptotic and reactive oxygen species (ROS) generation effects both in-vitro and in-vivo studies PLB induced apoptosis and autophagy by generating reactive oxygen species to mediate JNK and AKT/mTOR pathways.

(Singh et al., 2021) Reported that plumbagin involve increased oxidative stress, caspase activity, loss of mitochondrial membrane potential, induction of cytochrome c release, FasL expression, and high Bax levels via activation of the JNK pathway, down-regulation of expression of NF- κ B, suppressed TNF- α -induced phosphorylation of p65 and I κ B kinase (IKK), degradation of I κ B α , and blocking STAT3/ polo-like kinase 1 (PLK1)/AKT signaling

(Zhang et al., 2021) Reported that Plumbagin have effective cardioprotective activity against isoprenaline hydrochloride (ISO)-induced MI heart injury. Increased the antioxidative enzymes, and decreased the levels of pro-inflammatory cytokines (TNF- α , IL-6, and NF κ B) and reduced Na⁺/K⁺-ATPase activity Plumbagin pretreatment could reduce the ROS production by regulating the expression of NOX4 and down regulated NF- κ Bsignalling, and inhibit OGDR induced NLRP3 inflammasome activation.

(Jangra et al., 2021) Reported that ICV-LPS administra- tion causes memory impairment along with anxiety-like behavior in male Wistar rats. The mechanism involved in the neuroprotection of plumbagin may be partially due to alleviation of oxido-nitrosative stress, neuroinflammation, mitochondrial dysfunction and cholinergic deficits in the hippocampus. plumbagin could be a potential therapeutic phytochemical in neuropsychiatric illness associated with inflammation. previous study reported that plumbagin ICV-streptozotocin-induced memory deficits through activation of Nrf2/ARE in the hippocampus

(Nakhate et al., 2018) Suggested that Plumbagin improves cognitive deficits and astrogliosis in STZ induced mouse model of AD via Nrf2/ARE mediated suppression of astrogliosis and inhibition of β -secretase enzyme.Plumbagin inhibited A β ₂₅₋₃₅-induced oxidative stress by decreasing ROS and MDA, increasing Nrf-2, haemoxygenase 1 and NAD(P)H dehydrogenase quinone 1, and reducing NF- κ B, cyclooxygenase-2 (COX-2), and inducible nitric oxide synthase (iNOS) levels(**Wang et al.,2004**).

(Wang et al., 2004) Showed that plumbagin mediated the protective effect against A β ₂₅₋₃₅-induced neurotoxicity by suppressing redox imbalance and inflammation by down regulating NF- κ B and target genes with concomitant up regulation of Nrf-2 signaling.(**Yong et al., 2013**).Plumbagin ameliorates diabetic nephropathy via interruption of pathways that include NOX4 signalingneuroprotection by plumbagin involves BDNF-TrkB-P13K/Akt and ERK1/2

JNK pathways in isoflurane-induced neonatal rats ((**Yuan et al., 2017**). Plumbagin reduces EPC migration and tube formation by regulating the PLC, Akt, ERK, NF- κ B and HIF-1 signaling pathways (**Lee et al., 2019**)

(**Chen et al., 2018**) The anti-cancer activities of plumbagin are reported to be mediated via its ability to modulate the activity of multiple intracellular signaling proteins such as NF- κ B, AMPK, JNK, PI3K/Akt/mTOR signaling pathway and Wnt/ β -catenin. Chemically plumbagin is a naphthoquinone derivative. It is also commonly found in the carnivorous plant genera *Drosera* and *Nepenthes*. It is also a component of the black walnut drupe. Plumbagin has a hydroxyl group on the 5th position, which has the ability to trigger autophagy via inhibition of the Akt/mTOR pathway and which induces G2/M cell cycle arrest and apoptosis in A549 cells through JNK dependent p53 Ser15 phosphorylation. When the m-TOR inhibition occurs the cell division is arrested as which will lead to prevention of rapid cell growth inside the body.

(**Son et al., 2010**) Suggested that Plumbagin inhibited neuronal apoptosis in a rat model of cerebral ischemia via amplifying the anti-apoptotic (Bcl-2 and Bcl-XL) expression and diminishing the pro-apoptotic (Bad and Bax) and the cleaved caspase-3. Plumbagin increases ARE target gene (HO-1) levels in the cerebral cortex and striatum when administered intravenously and, when administered prior to focal ischemia/reperfusion, reduces brain cell damage and improves functional outcome in a mouse stroke model.

(**Dhingra et al., 2015**) Reported that In stressed mice, plumbagin produced antidepressant effect and increased the level of glutathione in the brain and reduce oxidative stress. A previous study showed the neuroprotective effect of Plumbagin against isoflurane-induced neuronal damage via ERK1/2/JNK and BDNF-trkb-PI3K/Akt pathways. Plumbagin ICV-streptozotocin-induced memory deficits through activation of Nrf2/ARE in the hippocampus (**Nakhate et al., 2018**) and carried out to reveal the neuroprotective effects of plumbagin against ICV-LPS induced behavioral and neuronal (**AshokJangra et al., 2021**). In previous studies molecular docking studies showed that plumbagin as better β -secretase inhibitor (binding energy (-10.03 kcal/mol)

(**BorhadePravin et al., 2013**) Plumbagin (RTK1), isolated from *Plumbago rosea* root extract that inhibits histone acetyltransferase activity potently in vivo. The root has a bitter taste and

laxative, expectorant, stomachic, tonic, abortifacient and appetizer property. The leaves are caustic and use in treatment of scabies.

(**Son T G, et al., 2010**) Revealed that treated mice with a daily intraperitoneal (i.p.) dose of plumbagin (0.5 and 1 mg/kg) starting from 1h prior to the first intracerebroventricularly treatment with streptozotocin (STZ; 3 mg/kg), a molecule able to recapitulate an AD-like condition. Plumbagin demonstrated the ability to prevent the loss of learning and memory in mice subjected to Morris water maze (MWM). They suggested that the anti-Alzheimer's effect of plumbagin could be associated with activation of Nrf2/ARE signaling with consequential suppression of astrogliosis and inhibition of BACE1. They confirmed their hypothesis with the administration of an Nrf2/ARE inhibitor. Finally, docking studies allowed the demonstration of the excellent binding mode of plumbagin to B and D chains of BACE1 enzyme. (**Campora et al., 2021**)

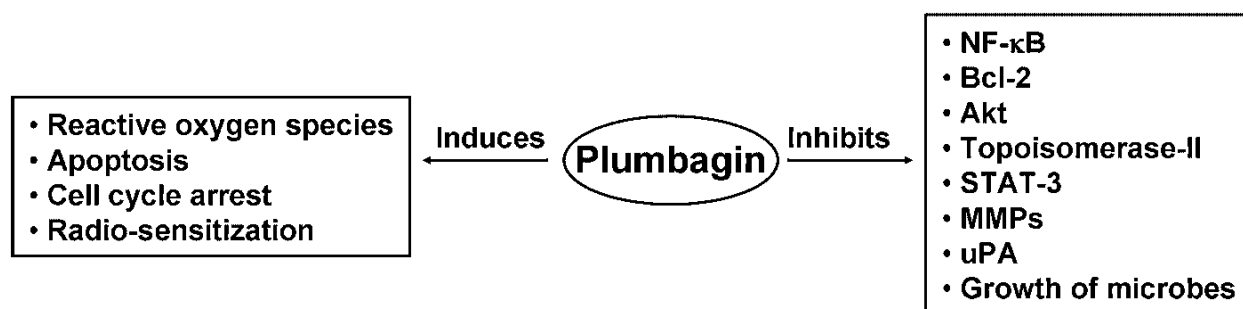


Figure 8: Summarization of molecular-biological effects of plumbagin. (**Rajalakshmi et al., 2018**)

Aim and Objectives

3. AIM AND OBJECTIVE

AIM

The aim of this study is to investigate the neuroprotective JNK3 inhibitory activity of plumbagin and its derivatives by using insilco computational methods.

OBJECTIVE

- To develop energetically minimized structure-based pharmacophore hypothesis for JNK3 inhibitors.
- To create database for plumbagin derivatives
- To screen the database with generated pharmacophore hypothesis
- To perform molecular docking for obtained compounds from database screening
- To compute the ADMET properties for selected HITS using Qikprop.
- To enumerate the binding free energy values for selected HITS using prime MM-GBSA.
- To assess the stability of the docked Protein-ligand complex using Molecular dynamics suite of Schrödinger V7.7.

Plan of Study

4. PLAN OF STUDY

PHASE-1

- Review of literature
- Selection of test compounds for docking study through literature
- The techniques and the protocols required for the study were optimized

PHASE-2

- Pharmacophore hypothesis generation
- *In silico* identification and screening of plumbagin derivatives with generated pharmacophore hypothesis
- Molecular docking studies of plumbagin derivatives from the screened database.
- Preliminary ADMET properties and MM-GBSA analysis
- Molecular dynamics simulation for the selected compounds

Materials and Methods

5. MATERIALS AND METHODS

INSILICO SCREENING:

Computational details:

In silico simulations like protein preparation, ligand preparation, grid generation, molecular docking, molecular mechanics were performed in Maestro 11.9.011 modeling package provided by Schrödinger, LLC, New York, NY, 2019-1, installed in Dell Optiplex 3060 with processor intel core i7-8700, Ubuntu 16.04 LTS, Graphics GeForce GT 730/PCIe/SSE2, and 64-bit OS. Energetically optimized structure-based Pharmacophore generation and molecular dynamics were performed in Maestro 12.4 modeling package provided by Schrödinger, LLC, New York, NY, 2020-2, installed in Dell precision 7820 with processor Intel Xenon(R) Gold 6130, Kernel GNOME Version 3.28.2 CentOS Linux 7, Graphics Quadro P5000/PCLe/SSE2 and 64-bit OS.

Protein Preparation:

The crystal structure of JNK3 was taken from RCSB PDB (Protein data bank) (PDB ID: 30Y1) Resolution 1.7Å. The selected co-crystallize structure was chosen based on low inhibitory binding activity and resolution of crystallized protein. Protein was prepared by using protein preparation.

Protein preparation process with three steps:

Import and pre-process review and modify and refine. In processing step bond orders were assigned, hydrogen bond is optimized, deletion of water outside from hot group creating zero bond order for disulfide bond conversion of selenomethionines to methionines if it present missing side chain & missing loops and in the JNK3 were identified. In the refine steps JNK3 co-crystallize structure was analyzed and unwanted hetro groups were removed. Epik V4.0 was used to generate possible ionization and tautomeric states for or all hetero groups at pH 7.0 + 2.0. The final step was done by minimizing the energy using the OPLS₃ force field with a default constrained of 0.30Å RMSD (or) energy minimization event was carried out to restrain the heavy atoms of 0.30Å, so that the stain can be relieved using force field OPLS3e. (Panwar et al., 2021).

Ligand Preparation:

Based on literature review plumbagin derivatives were selected and selected ligand (or) compounds was drawn using 2D sketcher. Ligprep was used to prepare ligand. Ligprep convert the 2D structure to 3D energy minimized molecular structure and also generate possible

stereoisomers, tautomers, ring conformation and possible states at physiological pH or any other were defined pH. By default, counter ions in salts and water molecules were removed charged groups were also neutralized by adding (or) eliminating hydrogen ions. Ionization states are generated using Epik V4.0 at a default pH is 7.0 + 2.0. Epik yields more accurate states, because it performs more sophisticated algorithm. Force field OPLS3e was used for energy minimization of each compound using Macromolecule V11.8 (Kalirajan et al., 2019)

Receptor grid generation:

After ligand and protein preparation the receptor grid was generated by using the receptor grid generation panel in GLIDE. The grid helps to define the receptor structure and determine the position and size of the active site. Receptor grid generation is an essential step if the protein was bounded to the ligand. In this step internal and external receptor grid boxes of 10×10×10Å and 20×20×20Å where defined force find energy used during the receptor grid generation was OPLS3e. The grid box was generated by centre of bound ligand as the centroid of the grid box in the receptor grid generation module of Glide 6.2 (Glide, Schrodinger, LLC, and New York, NY, USA). Ligand docking was carried out after grid generation.

Pharmacophore Hypothesis Generation

In this study, the phase module of Schrodinger was used for phamacophore hypothesis development. PHASEV3.8 is a highly flexible system for pharmacophore perception, structure alignment, activity prediction, and database searching. PHASE provides a built-in set of six pharmacophore features; hydrogen bond acceptors (A), hydrogen bond donors (D), hydrophobic groups(H), negatively ionizable groups(N), positively ionizable groups(P), and Aromatic rings(R). Here, a crystal structure (PDB code: 3OY1) of JNK3 complexed with a known inhibitor was employed to generate an energetically optimized structure-based pharmacophore model. In order to get the desired efficient hypothesis, representative features with catalytic importance were selected. After these operations, a structure-based pharmacophore model comprising the most important pharmacophoric features will be generated. (James et al., 2021)(

Database screening

The generated e-pharmacophore hypothesis was used as a 3D query for screening the database. The purpose of this screening was to retrieve novel and potential leads suitable for

further development. Conformers were generated for each molecule in the database using Create Phase database panel facilitated with ligand preparation and ligand filtering tabs which can be used to filter the ligands based on QikProp properties, Lipinski's rule, and reactive functional groups. The hypothesis was added to the database screen and screening was carried out using a Phase database screen tool called Phase Ligand Screening with the screening protocol implemented in Schrödinger having Best/Flexible search options. The retrieved compounds were filtered and further refined based on docking scores and better interactions using molecular docking study.

Molecular docking:

GLIDE V_{7.7} was used for Ligand receptor docking study. All the ligands were docked within the grid-generated area of the protein structure of the JNK3. The extra precision (XP) mode of docking was performed for the selection of top hit ligands. The core setting, constraints, and torsional constraints were kept as a default parameter. After docking based on G-score and docking score top scored compound were selected. The below mentioned formula is used by GLIDE to calculate docking score

$$\text{G-Score} = 0.05\text{VdW} + 0.15\text{Coul} + \text{Lipo} + \text{H-bond} + \text{Metal} + \text{ReWard} + \text{Rot-B} + \text{Site}$$

Were,

VdW -Van der Waals energy,

Coul -Coulomb energy,

Lipo -Lipophilic contact term,

H-bond -Hydrogen bond,

Metal -Metal binding term,

ReWard -Record other penalty term,

Rot-B - The penalty for freezing rotatable bonds and

Site - The polar interaction of the active site.

The docking score consists of a sum of the Glide score, measured from the XP scoring function. It is used for comparing different Ligands. (Singh et al., 2021)

Molecular mechanics-generalized born surface area

MM-GBSA was carried out by PRIME module of Maestro V11.4. Prime MM-GBSA (Molecular Mechanics/Generalized Born Model and Solvent Accessibility) was used to estimate the ligand binding energies and ligand strain energies for the series of plumbagin derivatives towards JNK3 using VSGB as an implicit solvent model, OPLS3e force field and other parameters were kept unchanged. The MM/GBSA calculations are used to estimate relative binding affinity (ΔG_{bind}) of ligands to the receptor (reported in kcal/mol). The binding energy was calculated based on the following equation.

$$\Delta G = G_{\text{complex (minimized)}} - [E_{\text{ligand (minimized)}} + E_{\text{Receptor (minimized)}}]$$

For MM-GBSA calculations, all the protein atoms were kept rigid while relaxing the atoms of the compounds. (Shridhar Deshpande et al., 2021)

ADMET property prediction

Qikprop V5.4 tool of Maestro V11.4 (schrodinger, LLC, NEWYORK, USA) was used to find the preliminary ADME properties of selected ligands. Qikprop application was used to filter the Ligands based on ADME characteristics. Qikprop gives many essential descriptors, which play an essential role in absorption, distribution, metabolism, excretion and toxicity. (Sharma et al., 2016)

The Qikprop predicted descriptor includes:

Rule of five- number of violations of Lipinski's rule of five (Molecular weight <500, QPlogPo/w <5, H-bond donor <5, H-bond acceptor <10). Number of branches of Jorgensen's rule of three, these define the bioavailability of orally active drugs and include predicted aqueous solubility QPlogS (range: -6.5 -0.5), predicted CaCo-2 cell permeability (a model for the gut blood barrier) QPPCaCo (range: <25 poor and >500 great) and number of metabolic reactions (range: 1-8), predicted CNS activity, predicted blood brain barrier partition coefficient log BBB (range: -3.0 -1.2), predicted apparent MDCK cell permeability in nm/sec (<2.5 poor and >500 greater) and predicted IC50 value for blockage of HERG K⁺ channel (>-5.1), predicted human oral absorption percentage in GI ($\pm 20\%$), should not be less than 25. Ligands which satisfied above mentioned properties were considered for the present study. (Singh et al., 2019)

Molecular Dynamics

The MD simulations are carried out using DESMOND V5.2, a module of Maestro V11.4. MD simulation stands alone as the fundamental computational tool to understand the ligand-induced conformational changes of protein active site.

The basic steps followed in DESMOND were,

- Preparation of structure for simulation
- Generation of solvated system
- Distribution of ions to neutralize the system
- Relaxation of the system using OPLS_2005 force field
- The setting of simulation parameters
- Running of simulations
- Analysis of results using Trajectory viewer

The top most ranking protein- ligand complexes was selected for 100 ns MD simulation using DESMOND V5.7 using the force field of OPLS_2005. MD simulation was initiated with building a model system using the system builder. SPC explicit water model and a distance of 10Å orthorhombic simulation box were selected using the salvation tab. The system was neutralized with a counter ion such as Na⁺ and Cl⁻ ion at a salt concentration of 0.15M. The resulting model system was subjected to a 100ns MD simulation using NPT ensemble class (pressure, temperature, constant number of particles). The resultant MD trajectory was analyzed for the stability of complex formation using different parameters such as RMSD, RMSF, SSE, percentage protein-ligand contacts, ligand torsion profile and compared with co-crystal complexes. **(Kumar et al., 2019)**

Results

6. RESULTS

PROTEIN VALIDATION:

In the current docking study, we have used previously mentioned crystal structure of JNK3 protein. This protein structure (PDB ID: 3OY1) was selected based on resolution and other statistical parameter of protein structure, such as R free, R-value. Protein was validated by redocking experiment. In the redocking experiment, the conformation of 5-[2-(cyclohexylamino)pyridin-4-yl]-4-naphthalen-2-yl-2-(tetrahydro-2H-pyran-4-yl)-2, 4-dihydro-3H-1, 2, 4-triazol-3-one was successfully reproduced, close to that of co-crystallized ligand conformation (Figure 9). The redocking conformation was aligned with the original inhibitor conformation using superposition tool to check root mean square deviation (RMSD) in order to confirm the accuracy of docking program and it was found to be 0.957 which is less than 1 is acceptable RMSD. Extra precision docking with receptor flexibility was used for all Glide docking runs with default settings. The protein was prepared using the protein preparation wizard. For the active site, a grid box centered at the ligand was used to accommodate a maximum ligand length of same as that of workspace ligand. Default values were accepted for Van der Waals scaling and positional constraints. Post docking minimization of ligands was also included with a default number of poses per ligand to produce better poses of ligand to the receptor.

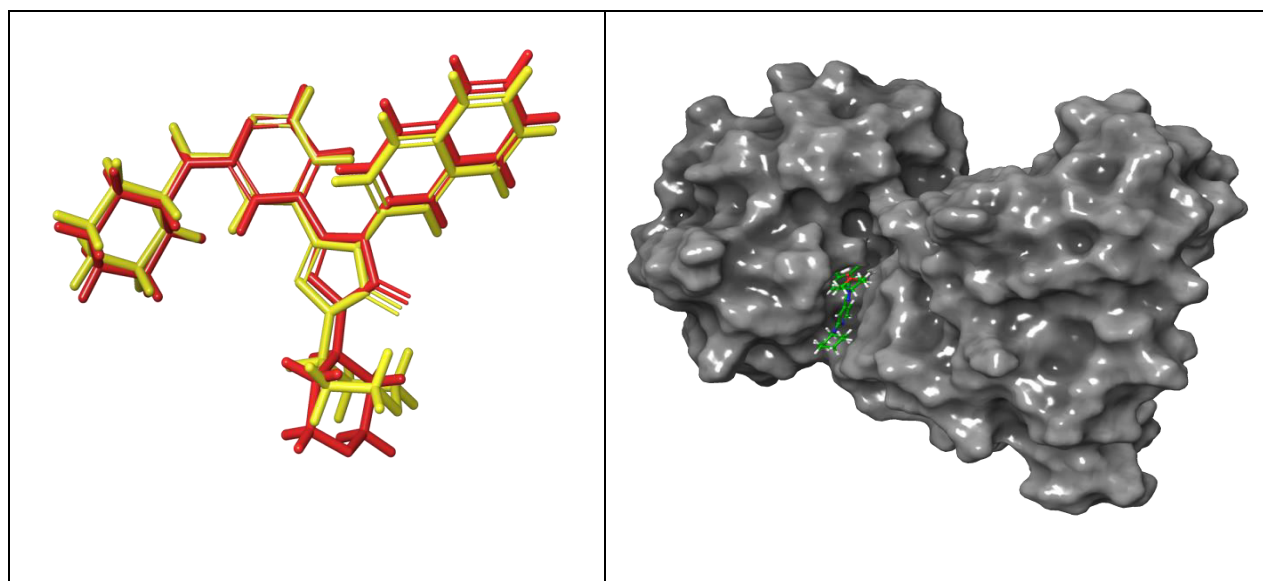


Figure 9: 3OY1 JNK3 protein validation-Alignment of redocked conformations.

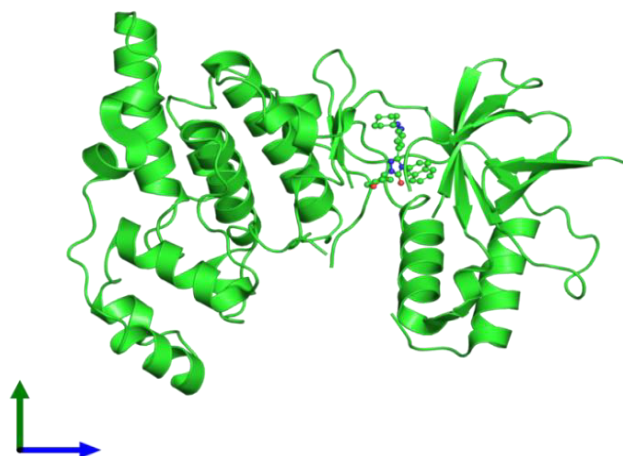
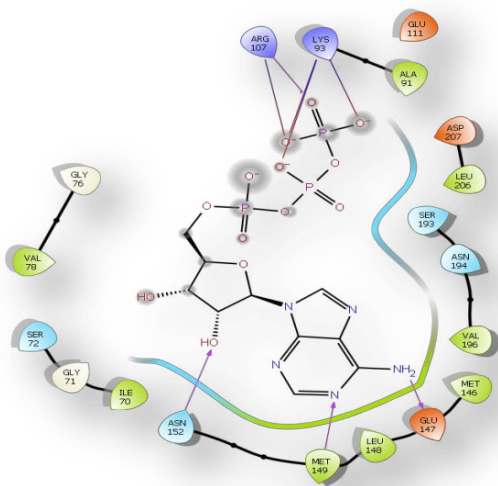


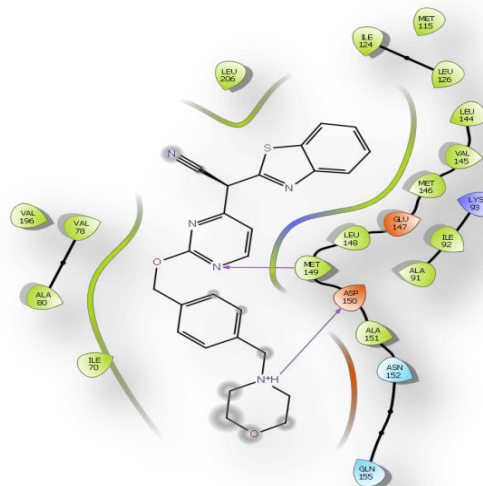
Figure 10: Ribbon diagram of the JNK3 protein (3OY1).

INVESTIGATION OF IMPORTANT AMINO ACID INTERACTION:

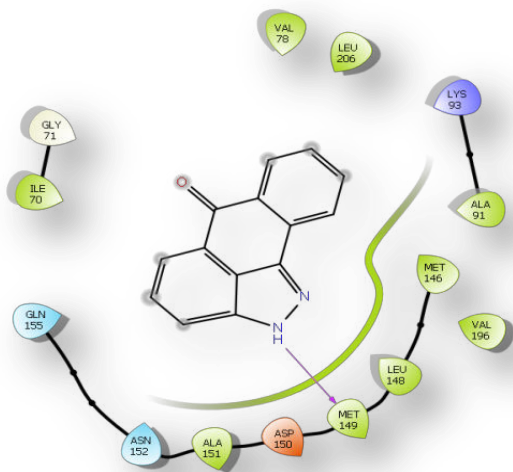
The important amino acid interactions and essential regions of the protein which is required for the ligands effective binding and activity were analyzed by performing molecular docking. Endogenous agonist ATP and five JNK3 inhibitors (SP600125, AS601245, CC-401, Bentamapimod, and CC-930) were docked with the above validated JNK3 (3OY1) protein and the common interactions were noted (Figure: 10). All the above-mentioned docking was performed in Extra Precision (XP) mode. XP visualizer module was utilized to analyze the docking results. The region required for the desired activity, which was shown as rewards and the region affecting the activity, which was shown as a penalty in the XP visualizer table was noted for effective pharmacophore feature selection. Docking score and common amino acid interaction of reference compounds shown in Table 1.



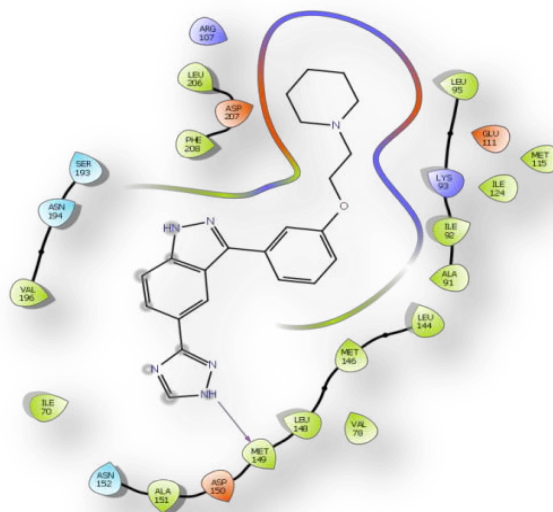
ATP



Bentamapimod



SP600125



CC-401

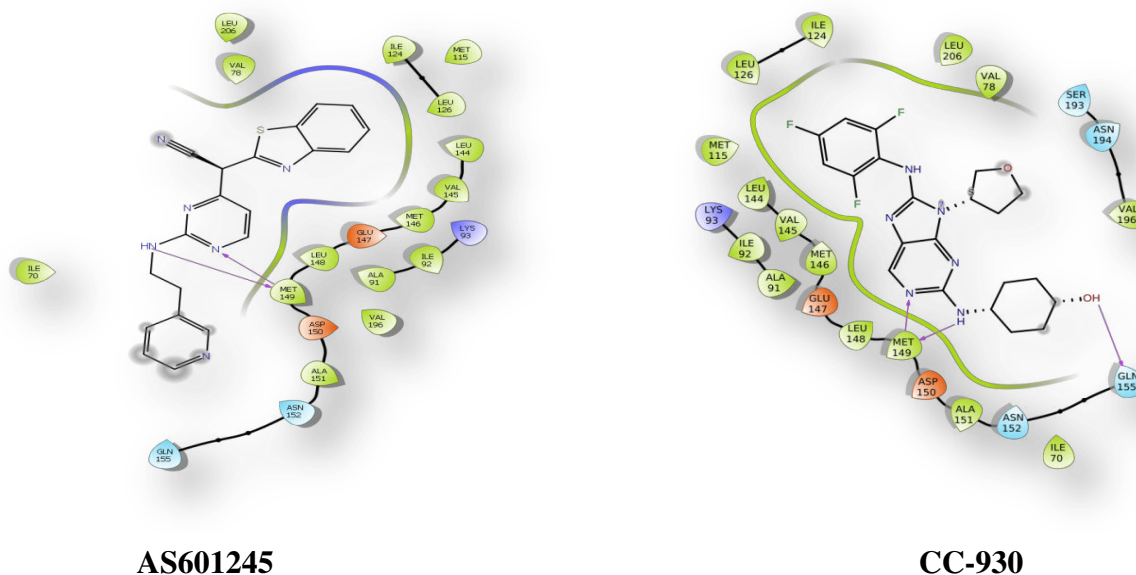


Figure 11: Interaction of ATP and JNK3 inhibitors with 3OY1

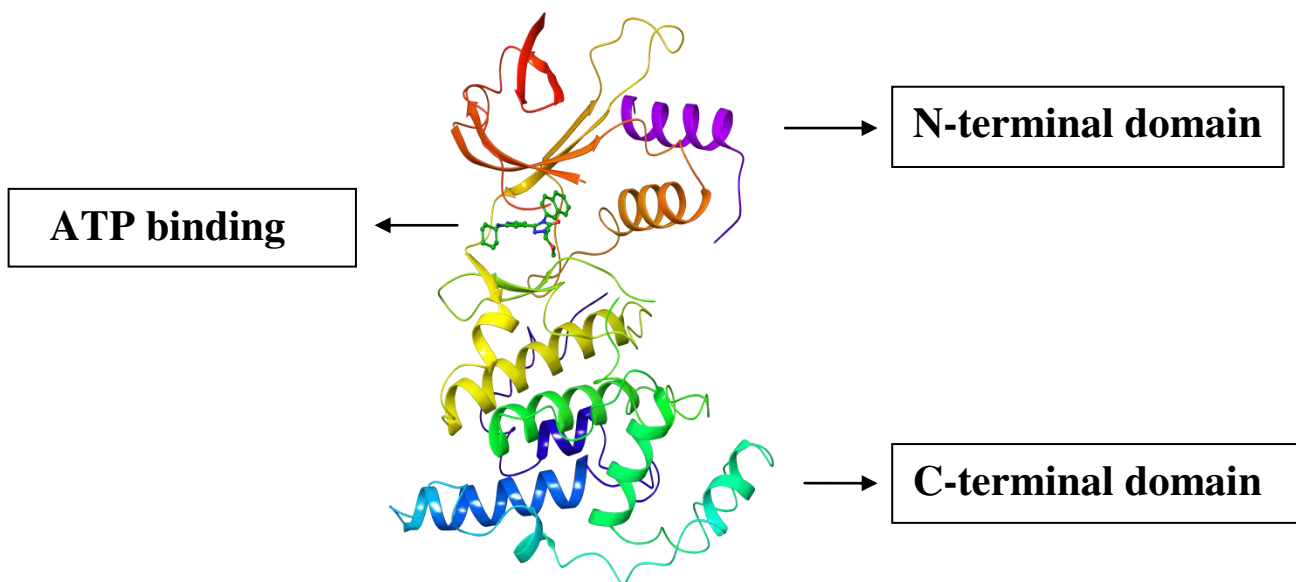


Figure 12: The N- terminal domain, C-terminal domain and activation loop

JNK3 has a typical kinase fold, with the ATP-binding site situated within a cleft between the N- and C-terminal domains. In contrast to other known MAP kinase structures, the ATP-binding site of JNK3 is well ordered; the glycine-rich nucleotide-binding sequence forms a β -strand–turn– β -

strand structure over the nucleotide. The N-terminal domain (residues 45–149 and 379–400) of JNK3 contains mostly β strands, whereas the C-terminal domain (residues 150–211 and 217–374) is predominantly α helical. A deep cleft between the two domains comprises the ATP-binding site, where the glycine-rich sequence (Gly71-Ser-Gly-Ala-Gln-Gly-Ile-Val78) of JNK3 forms a well-defined β -strand–turn– β -strand structure over the nucleotide.

Table 1:

Summary of G-score and common amino acid residues interaction in JNK3 protein (3OY1)

JNK3 INHIBITORS	G-SCORE	COMMON AMINO ACID RESIDUE INTERACTION IN JNK3	NATURE OF INTERACTION
SP600125	-7.840	MET 149	Hydrogen bond
AS601245	-9.045	MET 149	Hydrogen bond
CC-930	-10.112	MET 149 GLN155	Hydrogen bond Hydrogen bond
Bentamapimod	-7.112	MET 149 ASP 150	Hydrogen bond Hydrogen bond
CC-401	-6.471	MET 149	Hydrogen bond

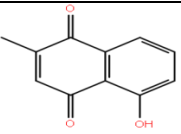
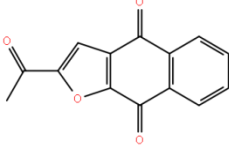
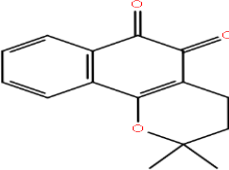
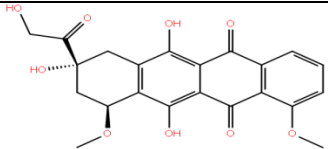
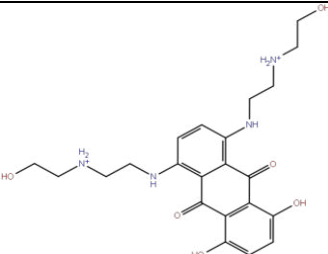
COMPOUNDS FOR HYPOTHESIS DEVELOPMENT:

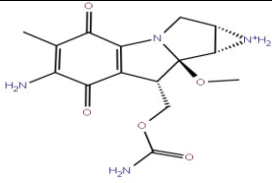
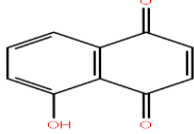
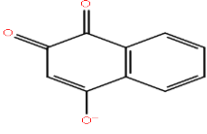
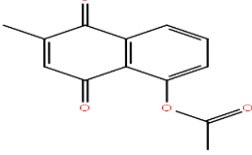
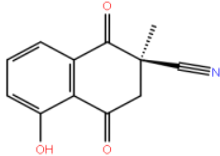
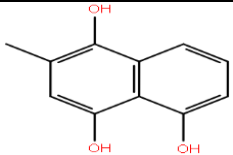
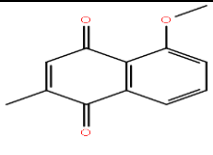
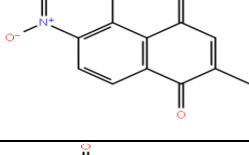
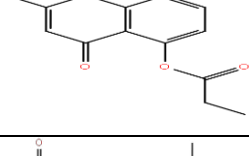
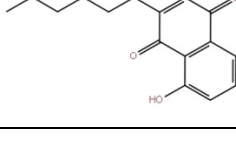
From the above mentioned three JNK3 inhibitors, were selected for pharmacophore hypothesis generation, these compounds selection based on docking score and also which is possess phase I, II clinical development. Three compounds namely SP600125, AS601245, CC-930, was found to have desired selectivity towards JNK3. Hence, these compounds were selected for pharmacophore hypothesis development.

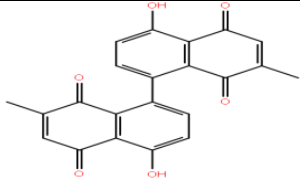
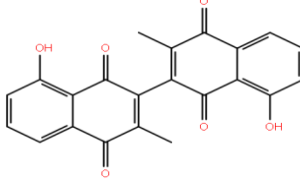
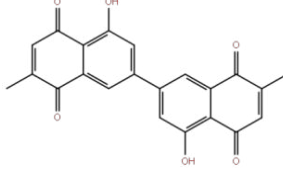
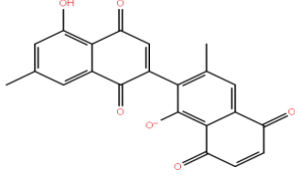
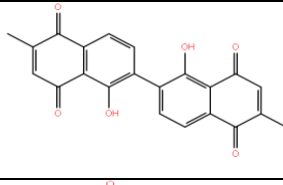
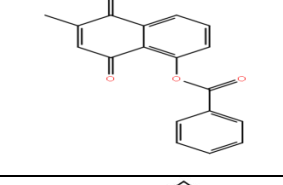
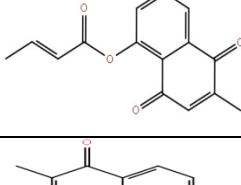
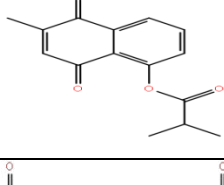
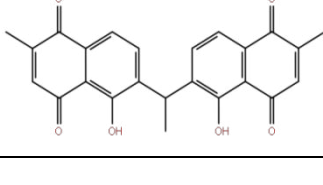
DATABASE CREATION:

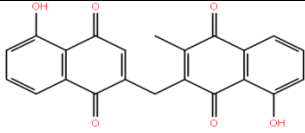
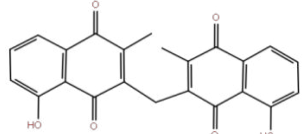
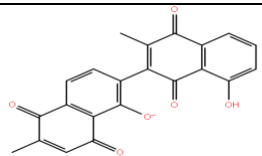
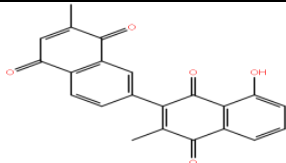
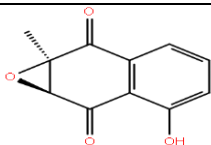
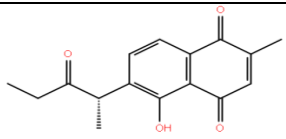
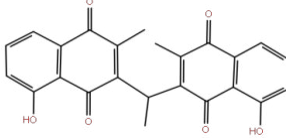
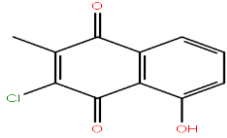
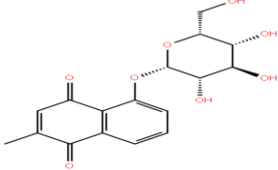
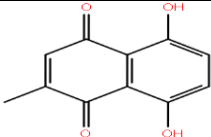
75 Plumbagin derivatives were retrieved from literature. These structures were drawn by using 2D sketcher. Database created for PLB derivatives using “CREATE PHASE DATABASE” module. The phase database creation processes comprise two steps, ligand preparation followed by ligand filtration. In ligand preparation, the molecules were converted from 2D chemical structure to 3D energy minimized molecular structure, salts were removed, possible stereoisomer and tautomers were generated as already described in Ligprep. In ligand filtration, the ligands were filtered based on Qikprop properties, Lipinski’s rule. This phase created database was taken for hypothesis screening. Structure activity relationship of plumbagin shown in Figure 7.

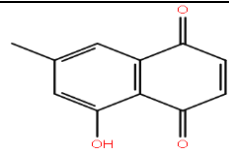
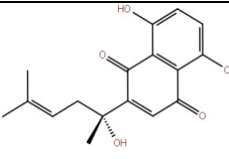
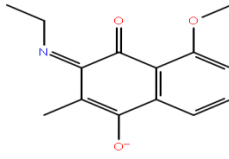
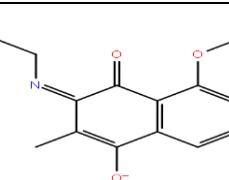
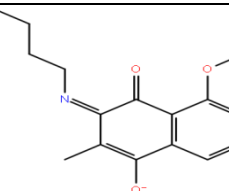
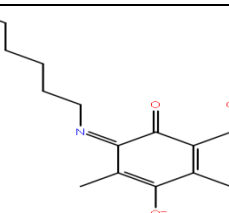
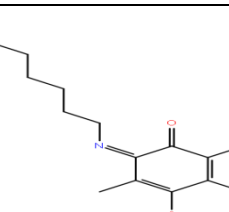
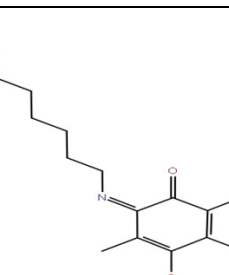
Table 2: Phase database compounds of Plumbagin derivatives and its structure

S.NO	COMPOUNDS	STRUCTURES OF COMPOUNDS
1	Plumbagin	
2	Napabucasin	
3	Beta-lapachone	
4	Doxorubicin	
5	Mitoxantrone	

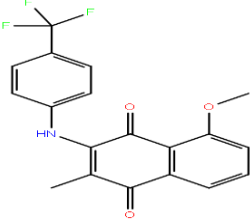
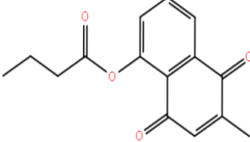
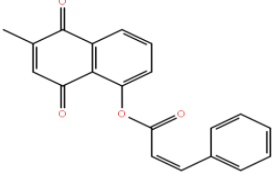
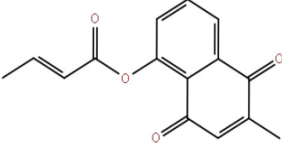
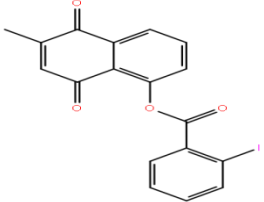
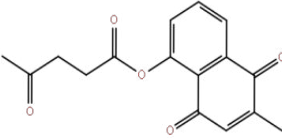
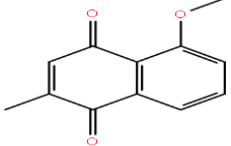
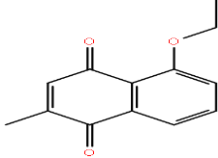
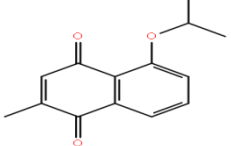
6	Mitomycin c	
7	Juglone	
8	Lawsone	
9	Acetyl plumbagin	
10	Cyano plumbagin	
11	Hydroquinonoid plumbagin	
12	Methyl plumbagin	
13	Nitro plumbagin	
14	Propionate plumbagin	
15	3-(5-oxohexyl) Plumbagin	

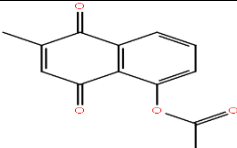
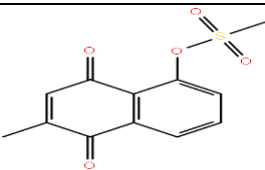
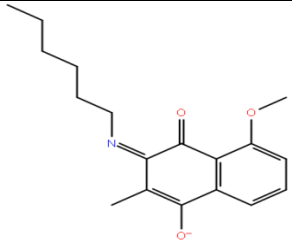
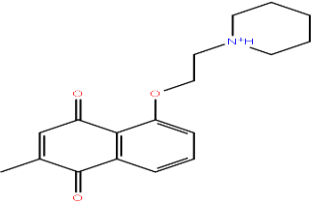
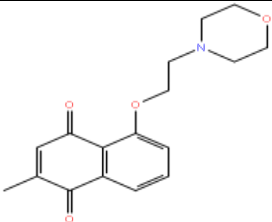
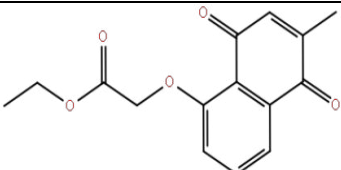
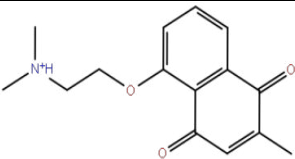
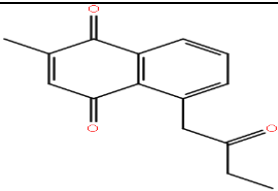
16	Maritinone	
17	3,3'-biplumbagin	
18	7,7'-biplumbagin	
19	Isodiospyrin	
20	Elliptinone	
21	Benzoate plumbagin	
22	Crotonate plumbagin	
23	Isobutyrate plumbagin	
24	Ethylidene 6,6'-biplumbagin	

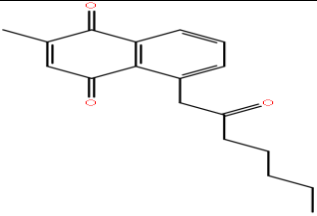
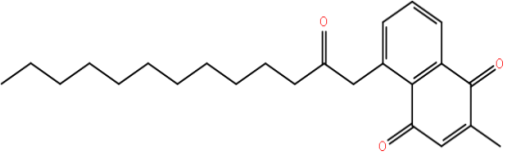
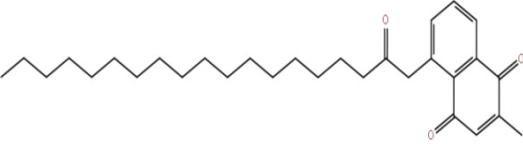
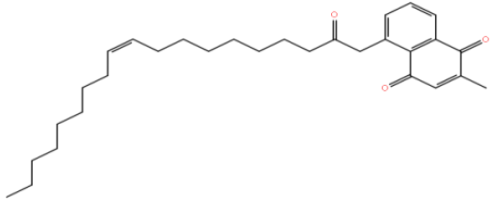
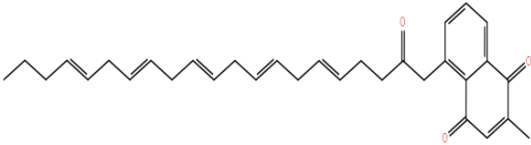
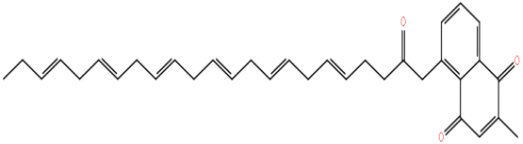
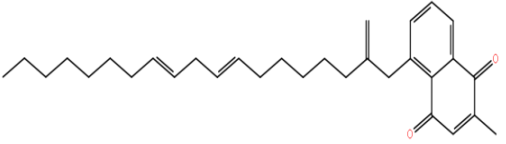
25	Isozeylanone	
26	Methylene-3,3'-biplumbagin	
27	Chitranone	
28	3,8'-biplumbagin	
29	2,3-epoxy plumbagin	
30	6-(1-ethoxyethyl)plumbagin	
31	Ethylidene 3,6' biplumbagin	
32	3-chloro plumbagin	
33	Plumbagin-5-o-glucoside	
34	Ramenton	

35	7-methyljuglone (Ramentaceon)	
36	Shikonin	
37	3-(Ethyl amino)-5-methoxy-2-methylnaphthalene-1,4-dione	
38	5-Methoxy-2-methyl-3-(propylamino)naphthalene-1,4-dione	
39	3-(Butylamino)-5-methoxy-2-methylnaphthalene-1,4-dione	
40	3-(Hexylamino)-5-methoxy-2-methylnaphthalene-1,4-dione	
41	5-Methoxy-2-methyl-3-(octylamino)naphthalene-1,4-dione	
42	5-Methoxy-2-methyl-3-(nonylamino)naphthalene-1,4-dione	

43	3-(Decylamino)-5-methoxy-2-methylnaphthalene-1,4-dione	
44	3-(Dodecylamino)-5-methoxy-methylnaphthalene-1,4-dione	
45	(E)-5-Methoxy-2-methyl-3-(octadec-9-enylamino)naphthalene-1,4-dione	
46	3-(Allylamino)-5-methoxy-2-methylnaphthalene-1,4-dione	
47	3-(Benzylamino)-5-methoxy-2-methylnaphthalene-1,4-dione	
48	3-(4-Fluorobenzylamino)-5-methoxy-2-methylnaphthalene-1,4-dione	
49	5-Methoxy-3-(4-methoxybenzylamino)-2-methylnaphthalene-1,4-dione	

50	5-Methoxy-2-methyl-3-(4-(trifluoromethyl)benzylamino)naphthalene-1,4-dione	
51	Butyrate plumbagin	
52	Cinnamate plumbagin	
53	Crotonate plumbagin	
54	Iodobenzoateplumbagin	
55	Levulinoate plumbagin	
56	5-Methoxy-2-methyl-1,4-naphthoquinone	
57	5-Ethoxy-2-methyl-1,4-naphthoquinone	
58	5-Isopropoxy-2-methyl-1,4-naphthoquinone	

59	6-Methyl-5,8-dioxo-5,8-dihydronaphthalen-1-ylAcetate	
60	6-Methyl-5,8-dioxo-5,8-dihydronaphthalen-1-ylMethanesulfonate	
61	3-(Hexadecylamino)-5-methoxy-2-methylnaphthalene-1,4-dione	
62	2-Methyl-5-(2-piperidin-1-ylethoxy)-1,4-naphtho-quinone	
63	2-Methyl-5-(2-morpholin-4-ylethoxy)-1,4-naphthoquinone	
64	Ethyl [(6-Methyl-5,8-di-oxo-5,8-dihydronaphthalen-1-yl)-oxy]acetate	
65	5-[2-(Dimethylamino)-ethoxy]-2-methyl-1,4-naphthoquinone	
66	5-O-propanolyloxy-2-methyl-1,4-naphthoquinone	

67	5-O-hexanoyloxy-2-methyl-1,4-naphthoquinone	
68	5-O-dodecanoyloxy-2-methyl-1,4-naphthoquinone	
69	5-O-octadecanoyloxy-2-methyl-1,4-naphthoquinone	
70	5-O-oleoyl-2-methyl-1,4-naphthoquinone (C18:1-Acyl plumbagin, 2f)	
71	5-O-eicosapentaenoyloxy-2-methyl-1,4-naphthoquinone	
72	5-O-docosahexaenoyloxy-2-methyl-1,4-naphthoquinone	
73	5-O-linoleoyloxy-2-methyl-1,4-naphthoquinone	

HYPOTHESIS GENERATION FOR THREE COMPOUNDS

Energetically optimized structure-based pharmacophore hypothesis was generated for selected three compounds from their corresponding retrieved frames. Manual hypothesis generation method opted in favour of selecting more desired features based on the interaction data collected from XP-visualiser table. Preferably, the regions which were shown as rewards in the XP-

visualiser table were selected first and other than that the features which are responsible for producing essential interactions were also selected. The generated three hypotheses were incorporated for database searching.

The SP600125 hypothesis contains two features including one hydrogen bond donor (D3) and one aromatic ring (R5) which is shown in **Figure 13**

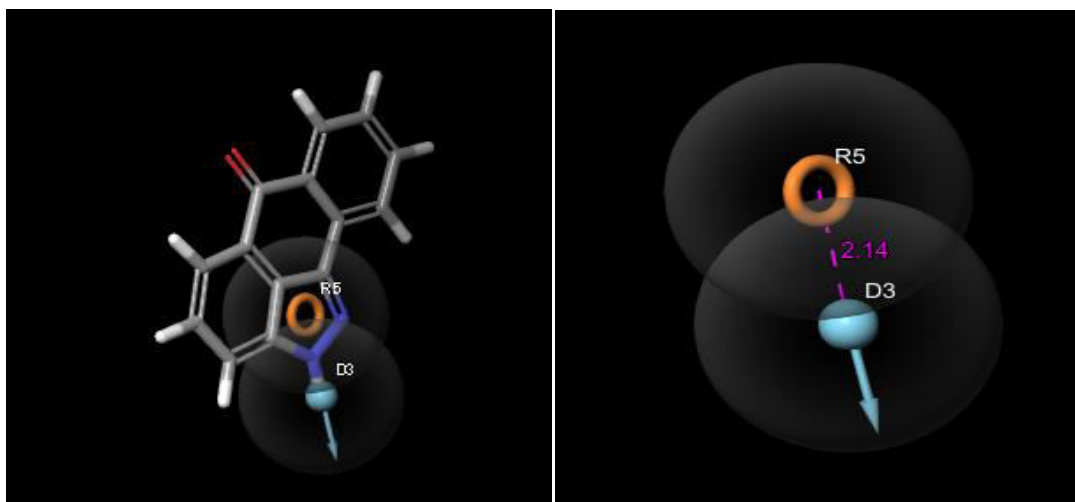


Figure13: A)generated e-pharmacophore hypothesis AD and B) inter site distance between the pharmacophoric sitesin Å spheres, Orange open circle, aromatic ring (R), blue sphere with arrow, hydrogen bond donor (D)

The AS601245 hypothesis comprises three features including), one hydrogen bond donor (D6) and one aromatic ring (R10) which is hydrogen bond acceptors (A5)shown in **Figure14**

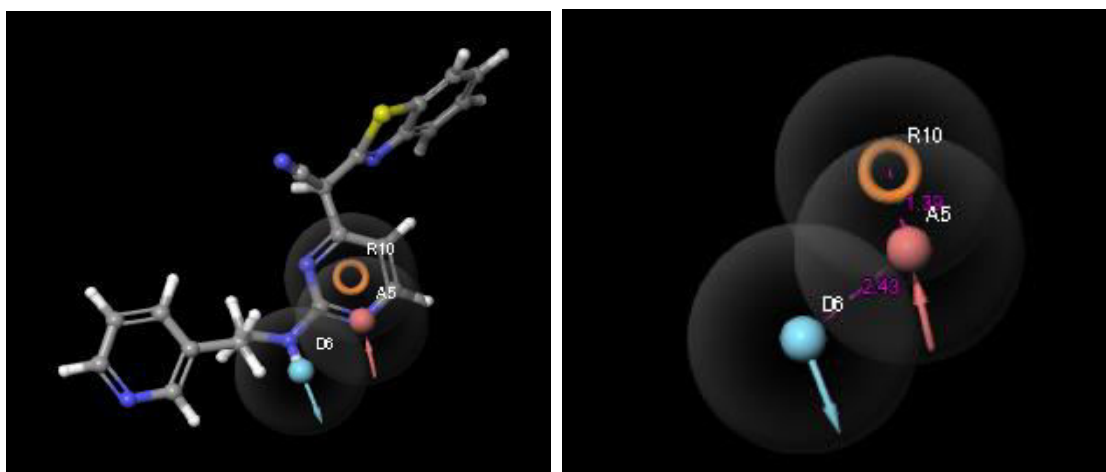


Figure 14: A) generated e-pharmacophore hypothesis ARD and B) inter site distance between the pharmacophoric sites in Å spheres, pink spheres with arrow, hydrogen bond acceptor (A) Orange open circle, aromatic ring (R), blue sphere with arrow, hydrogen bond donor (D)

The CC-930 hypothesis comprises four features including one hydrogen bond acceptor (A3), two hydrogen bond donors (D7, D6) and one aromatic ring (R15) which is shown in **Figure15**

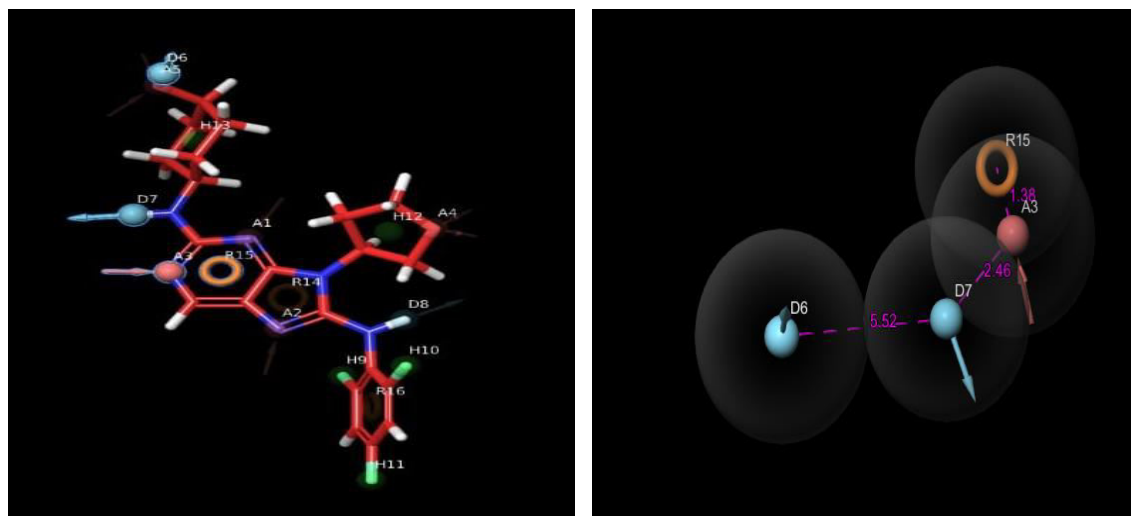


Figure 15: A) generated e-pharmacophore hypothesis ARDD and B) inter site distance between the pharmacophoric sites in Å spheres, pink spheres with arrow, hydrogen bond acceptor (A) Orange open circle, aromatic ring (R), blue sphere with arrow, two hydrogen bond donor (D)

DATABASE SCREENING FOR THREE HYPOTHESIS:

The generated pharmacophore hypothesis was put through database screening. Each hypothesis was screened with phase created DATABASE. This screening experiment was carried out in order to gain new compounds with potential inhibitory activity towards JNK3. SP600125 hypothesis was added to the phase database screen and 2 out of 2 features were fixed as minimum matching criteria. As a result of screening, 67 compounds were obtained. AS601245 hypothesis screening was done with 3 out of 3 features as minimum matching criteria. In this, 54 compounds were received. Likewise, CC-930 hypothesis was screened separately with fixing 4 out of 4 as a minimum matching requirement. Here, 48 compounds were screened.

MOLECULAR DOCKING:

Molecular docking is a Structure-Based Drug Designing method used to understand the molecular interaction of ligand and target. Molecular docking study reveals binding site topology, including the presence of clefts, cavities, sub-pockets, and electrostatic properties, such as charge distribution. Careful analysis of molecular interaction could facilitate the design of the ligands possessing the necessary features for efficient binding with the target receptor, thus leading to achieve desired pharmacological and therapeutic effects. Here, Insilco molecular docking simulation was conducted of plumbagin derivatives which were obtained from above the hypothesis screening were taken for molecular docking inspection and their binding energies were calculated. Glide score, Fitness score, align score binding energy, number of hydrogen bond interactions, bond length, and amino acids involved in the interactions are shown in Table 3. 57 compounds obtained from SP600125 hypothesis, 43 compounds obtained AS601245, 22 compounds obtained from CC-930 hypothesis were docked with JNK3(3OY1) protein in the extra precision mode (XP). Which are then filtered basis of interactions and docking score. All the docked compounds were fit on the enzyme active site with the highest docking score in the range of -7.740 to -10.688 kcal/mol. After interaction analysis, we found that compounds acquire primary common interactions of MET149. Which completed the analysis of ligand binding confirmation with accurate amino acid interactions and docking score of the screened compounds were summarized in table 3. The final results of XP with the highest docking score were subjected to MD simulation.

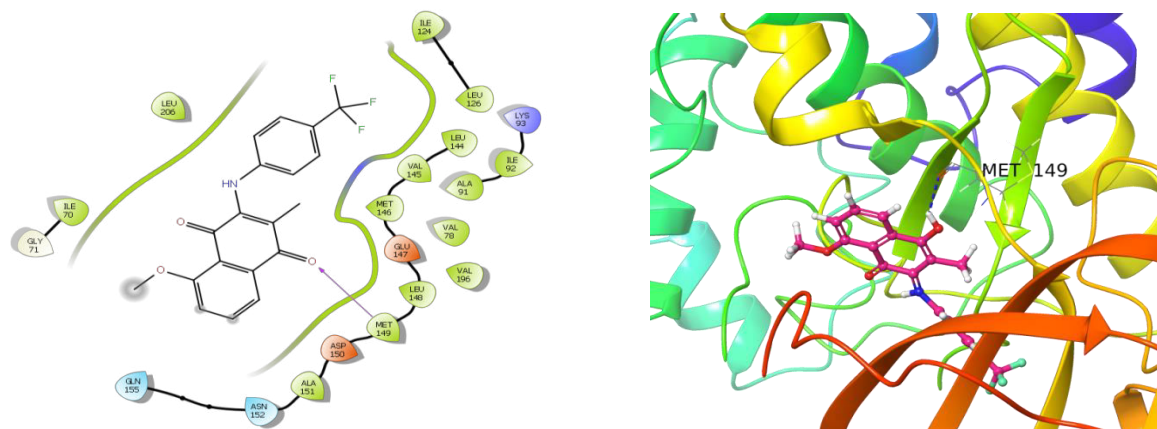


Figure 16 : 2D and 3D interaction diagram of 5-Methoxy-2-methyl-3-(4-(trifluoromethyl)benzylamino) naphthalene 1,4-dione from SP600125 hypothesis

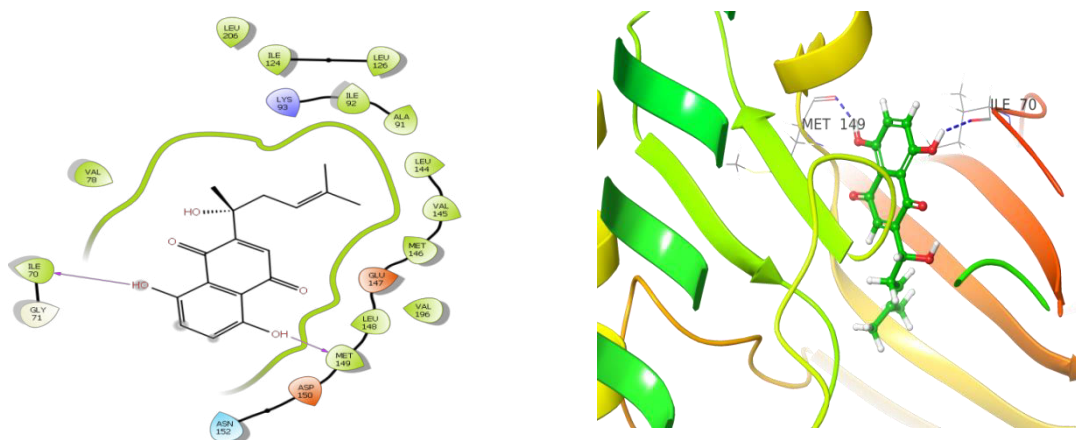


Figure17: 2D and 3D interaction diagram of Shikonin from AS6001245 and CC-930 hypothesis

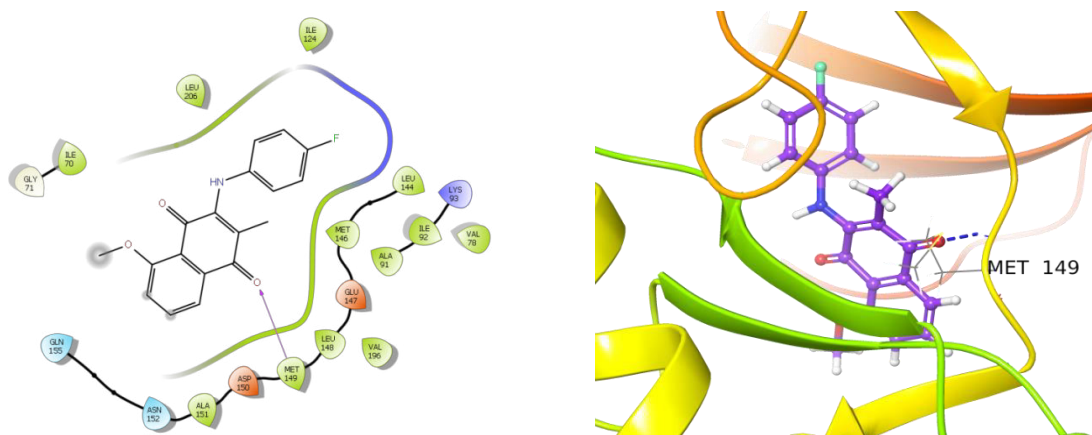


Figure 18: 2D and 3D interaction diagram of 3-(4-Fluorobenzylamino)-5-methoxy-2-methylnaphthalene-1,4-dione , from SP600125 hypothesis



Figure 19: 2D and 3D interaction diagram of Plumbagin-5-o-glucoside, from AS6001245 and CC-930 hypothesis

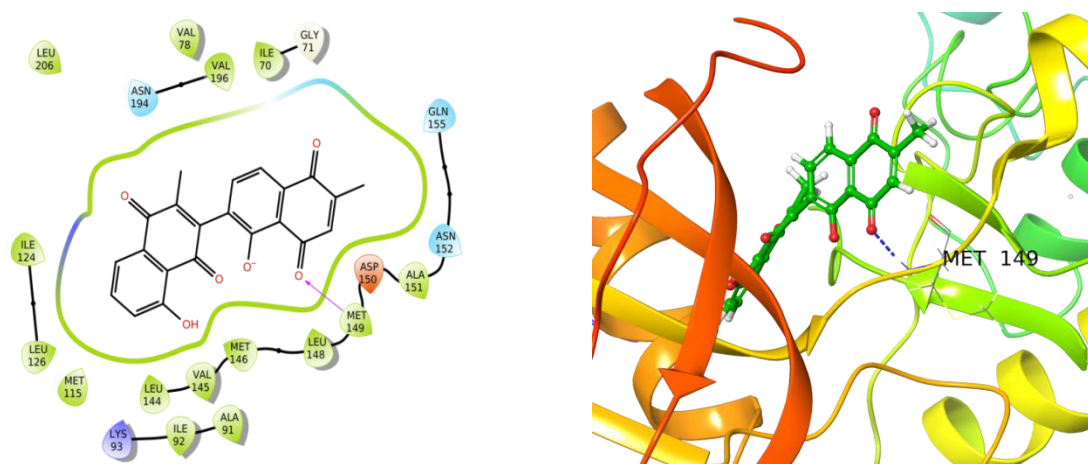


Figure 20: 2D and 3D interaction diagram of Chitrone from SP600125 hypothesis

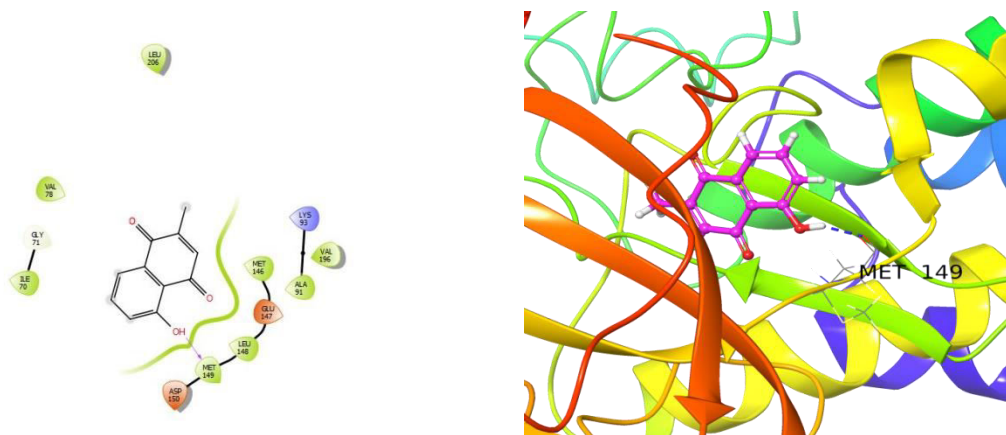


Figure 21: 2D and 3D interaction diagram of plumbagin from AS6001245 hypothesis

Table 3: Pharmacophore and glide docking results for best G-score compounds from hypothesis (SP600125, AS6001245, and CC-930)

Hypothesis 1 :SP600125						
S.No	Compounds	G-score	Align score	Fitness score	H-bond interaction	H-bond distance
1	5-Methoxy-2-methyl-3-(4-(trifluoromethyl)benzylamino)naphthalene1,4-dione	-10.522	0.88	1.16	MET149	2.09Å
2	3-(4-Fluorobenzylamino)-5-methoxy-2-methylnaphthalene-1,4-dione	-9.241	0.54	0.43	MET149	1.95Å
3	Chitranone	-8.999	0.67	0.57	MET149	2.39Å
Hypothesis 2: AS6001245						
5	Plumbagin	-7.740	0.67	0.36	MET149	1.71Å
	Shikonin	-10.688	1.24	0.88	MET149 ILE70	2.14Å 2.22Å
6	Plumbagin-5-o-glucoside	-9.046	0.58	0.93	MET149 ILE70	1.99Å 1.76Å
Hypothesis 3: CC-930						
7	Plumbagin-5-o-glucoside	-5.046	0.45	0.21	MET149 ILE70	1.99Å 1.76Å

No compounds were selected from CC-930 hypothesis as the compounds screened were similar to that of those screened in other hypothesis, moreover the compounds docked in this hypothesis have G-score very low when, compared to SP600125 and AS6001245 hypothesis.

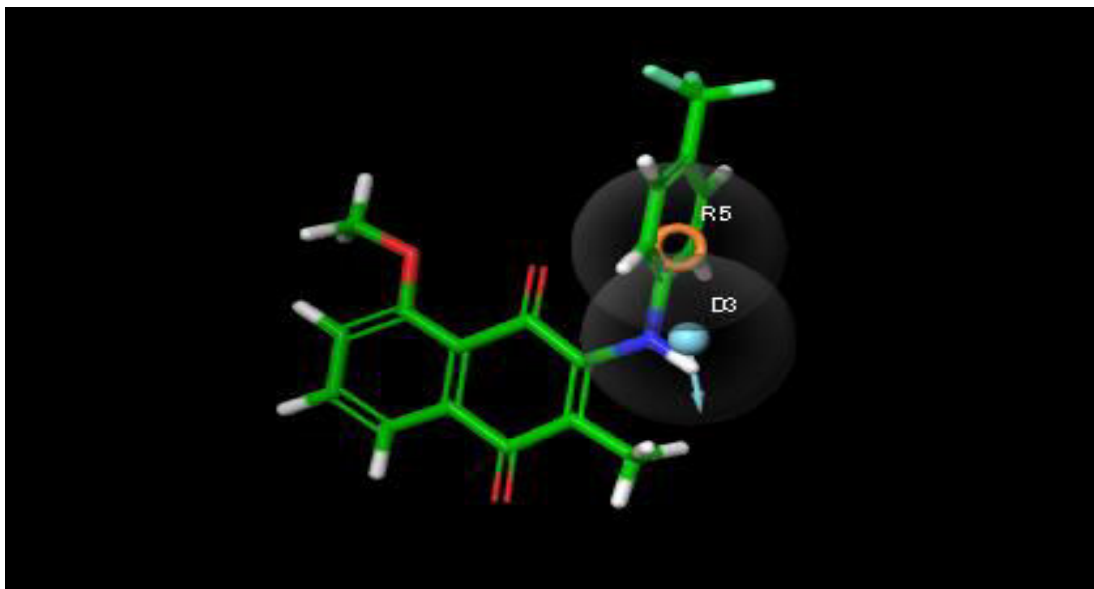
OVERLAP OF SELECTED COMPOUNDS WITH THEIR CORRESPONDING PHARMACOPHORE HYPOTHESIS

Figure 22: Overlay of 5-Methoxy-2-methyl-3-(4-(trifluoromethyl)benzylamino)naphthalene 1,4-dione with SP600125 hypothesis

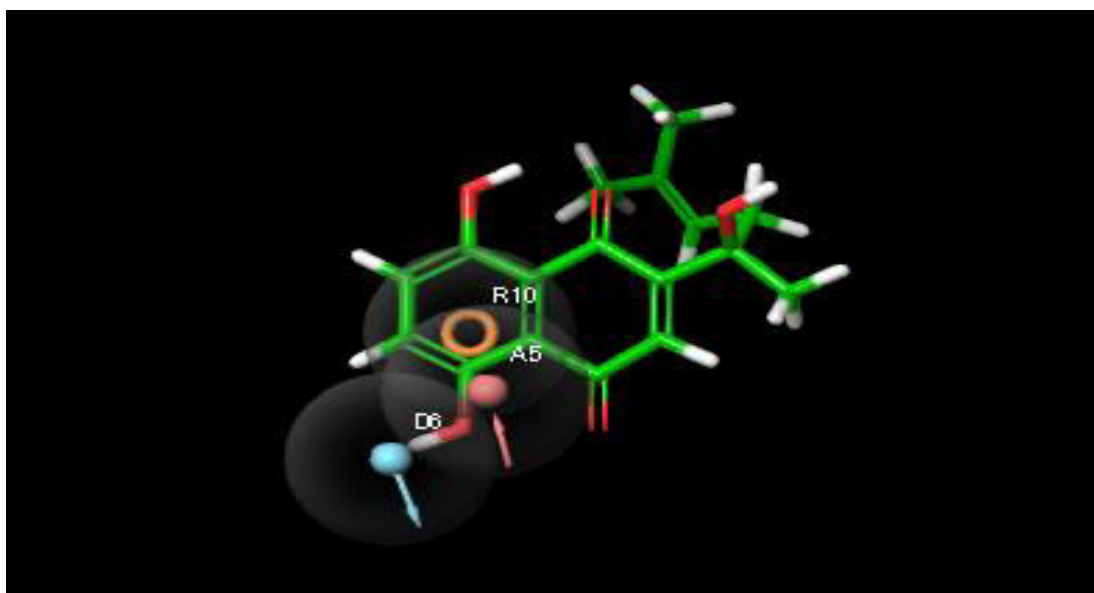


Figure 23: Overlay of Shikonin with AS6001245 hypothesis

PHARMACOKINETIC PARAMETER EVALUATION:

In drug discovering the ADME profile of drug like molecules is very important and for this purpose Schrodinger's maestro molecular modeling Qikprop module was utilized. Qikprop module of Schrödinger was used to analyze the drug likeness (Lipinski's rule of five) and

ADME (absorption, distribution, metabolism, excretion) evaluation of identified JNK3 inhibitors and plumbagin derivatives, which demonstrated physically significant descriptors and pharmaceutically relevant properties (ADME) of the ligand. The predicted drug likeness descriptors such as QPPCaco, QPLog HERG, LogP MDCK, QP log BB, QP log S and percentage of Human oral absorption were given in Table 4. Moreover, analyzed the ADME properties of these compounds; QPlog_{po/w} is the partition coefficient ranging from 0.79 to 3.94, which is crucial for the absorption and distribution estimation of drugs within the body, while QPPCaco is a cell permeability factor that determines the metabolism of a drug. The biological membrane access ranges from 51.419 to 1974.752, and Predicted IC₅₀ value for blockage of HERG K⁺ channels concern below -5 (range from -3.77 to -4.94). Aqueous solubility, Q log S, should be in the range from -1.023 to -5.453. The compounds have % Human oral absorption in the scope of 50.86 to 100%. Analyzing Lipinski's rule of five for plumbagin derivatives compounds exhibited no violations for molecular weight, hydrogen bond donors, and acceptors. The results of ADME studies indicate that all the compounds are within an acceptable range of Lipinski's rule of 5.

Analysis of blood/brain partition coefficient

Blood–brain barrier is a major hindrance to delivery of drugs to central nervous system. A low molecular weight and high degree of lipophilic molecule can cross the barrier easily. Too polar compounds cannot cross the membrane. In *insilico* analysis, QP log BB and QPMDCK parameters are used to assess the Blood–Brain partition coefficient. MDCK (Madin-Darby canine kidney) is good representative to mimic blood–brain barrier. Hence this was used to predict the cell permeability. Recommended range of QP log BB and QPMDCK is – 3.0 to 1.2 and < 25 (poor permeability), >500 (great permeability), respectively. Table 4 shows number of compounds falling within the standard range of QPlogBB and QPMDCK, which is an important precondition for a drug entering into central nervous system (CNS). The range of QP logPMDCK are from 35.009 to 4219.862. Analysis of QPMDCK showed that compounds A, B, C showed good permeability compared to others. Hence, these are too lipophilic and highly permeable for MDCK cells (Table 4).

Overall, the pharmacokinetic properties of identified compounds might act as drug like molecules. So from the results of *insilico* ADMET screening most of the compounds are within the recommended values.

Table 4: Qikprop results for reference compounds and top 5 plumbagin derivatives

S. No	Compounds	QP log S	QP log-HERG	QPP CaCo	QP log BB	QPPM -DCK	% Human Oral Absorption
1	Compound A	-5.453	-4.579	1848.9	-0.087	4219.8	100%
2	Compound B	-3.726	-4.152	276.74	-1.223	623.39	88.17%
3	Compound C	-4.208	-4.236	1974.4	-0.183	1864.6	100%
4	Compound D	-2.087	-4.652	51.419	-2.090	35.009	55.86%
5	Compound E	-3.48	-5.34	55.801	-1.824	55.854	66.45%
6	PLB	-1.386	-3.775	481.11 3	-0.611	224.33 5	79.641%
7	SP600125	-2.85	-4.490	992.49	-0.28	490.69	95%
8	AS60125	-1.023	-4.641	618.31	-1.06	498.48	100%

Table 5: Lipinski properties of compounds using Qikprop

S.NO	COMPOUNDS	Molecular weight	Dipole	Donor HB	Accept HB	QlogPo/w	Rule of Five
1	Compound A	361.320	4.405	1.00	5.25	3.945	0
2	Compound B	302.326	2.752	0.00	3.25	2.993	0
3	Compound C	311.312	2.509	1.00	5.25	3.104	0
4	Compound D	350.324	7.09	4.00	9.25	1.145	0

5	Compound E	374.112	1.6	0.00	7.0	1.409	0
6	PLB	188.182	2.58	0.00	3.75	0.795	0
7	SP600125	220.230	4.28	1.0	3.0	2.50	0
8	AS60125	457.549	7.35	0.0	8.7	3.57	0

Compound A- 5-Methoxy-2-methyl-3-(4-(trifluoromethyl) benzylamino) naphthalene1, 4-dione

Compound B- Shikonin

Compound C- 3-(4-Fluorobenzylamino)-5-methoxy-2-methylnaphthalene-1, 4-dione

Compound D- Plumbagin-5-o-glucoside

Compound E- Chitranone

MOLECULAR MECHANICS STUDY FOR SELECTED COMPOUNDS:

The combined Molecular Mechanical/Generalized Born Surface Area (MM/GBSA) approach is the fastest force-field based method that computes the free energy of binding from the difference between the free energies of the protein, ligand, and the complex in solution. The MM/GBSA method is based on the concept that the combination of molecular mechanics (MM) energies, polar and nonpolar solvation terms, and an entropy term can correctly render an approximate free energy of binding of a ligand to a receptor. Prime MM-GBSA approach was applied to predict the binding free energies (ΔG_{bind}) of top 5 compounds identified from Glide XP docking. The Prime MM-GBSA method was calculated by the free energy (ΔG_{bind}) of the selected inhibitors against JNK3 protein. In Glide docking, XP docking poses were obtained to perform MM-GBSA calculation and this was done using surface area energy, solvation energy, and energy minimization of the protein ligand complexes. The resulting MM-GBSA (ΔG_{bind}) ranging between -18.45 to -35.42 kcal/mol. The generated energy properties of selected compounds and native compounds were shown in (Table: 5) Among these, we found that the specifically screened compounds 5-Methoxy-2-methyl-3-(4-(trifluoromethyl)benzylamino)naphthalene1,4-dione and shikonin have the highest binding free energy in the negative range -35.42 kcal/mol and -32.13 kcal/mol relative to others, including reference compounds

Table 6: prime MM-GBSA energy properties of selected compounds and corresponding reference compounds

COMPOUNDS NAMES*	MM GBSA dG bind ^a	MM GBSA dG bind lipo ^b	MM GBSA dG Bind H bond ^c	MM GBSA dG Bind covalent ^d	MM GBSA dG bind Coulomb ^e	MM GBSA dG bind VdW ^f
5-Methoxy-2-methyl-3-(4-(trifluoromethyl)benzylamino)naphthalene-1,4-dione	-35.42	-5.64	-0.15	0.73	-11.10	-14.11
Shikonin	-32.13	-4.01	-0.70	0.85	-18.21	-11.31
3-(4-Fluorobenzylamino)-5-methoxy-2-methylnaphthalene-1,4-dione	-19.68	-7.24	-0.85	4.61	-20.32	-19.74
Plumbagin-5-o-glucoside	-25.86	-6.39	-0.68	0.36	-10.81	-19.50
Chitranone	-30.32	-6.22	-1.31	3.61	-19.86	-14.25
Plumbagin	-18.45	-2.26	-0.02	1.28	-38.30	-11.75
SP600125	-27.45	-3.41	-2.31	2.44	-14.76	-12.45
AS60125	-31.52	-1.53	-0.98	4.58	-11.45	-18.67

(Energy properties were measured in Kcal/mol)

* Values:

a- Free binding energy.

b- The surface area due to lipophilic energy contribution to the binding free energy (nonpolar contribution estimated by solvent accessible surface area).

c- Hydrogen bonding correction

d- Covalent energy contribution to the binding free energy

e- Coulomb energy contribution to the binding free energy.

f- Vander Waals energy contribution to the binding free energy.

MOLECULAR DYNAMICS:

In order to further verify the molecular docking result and whether the new inhibitors could bind to JNK3. The molecular dynamics simulation was carried out for the protein JNK3 with highest docking score compounds such as 5-Methoxy-2-methyl-3-(4 (trifluoromethyl) benzylamino) naphthalene1,4-dione and Shikonin. The protein-ligand complex was immersed in the orthorhombic box with SPC water solvent model for simulations using OPLS3e force field. After solvent system created, the simulations were equilibrated for 100 nanoseconds by Molecular Dynamics application.

MD simulation was conducted to find out the stability, conformation, and intermolecular interactions between the Ligands and active residues of the JNK3 protein over a 100-ns interval using the Desmond package. The generated MD simulation trajectories of each complex were subjected to specific parameters such as last pose analysis, root mean square deviation (RMSD), root mean square fluctuation (RMSF), and protein–ligand interaction profile to understand the bonding nature of the respective ligand at the active pocket of protein during simulation interval. A molecular dynamics simulation study was necessary to examine the stability and dynamic fluctuations in the ligand-protein complex under a simulated biological environment.

Protein-ligand interaction of the compounds such as **5-Methoxy-2-methyl-3-(4-(trifluoromethyl)benzylamino) naphthalene1,4-dione** and **shikonin** have been examined during course of MD simulation.

PL-RMSD: protein-ligand root mean square deviation this is used to measure scalar distance for the protein and ligand throughout the trajectory.

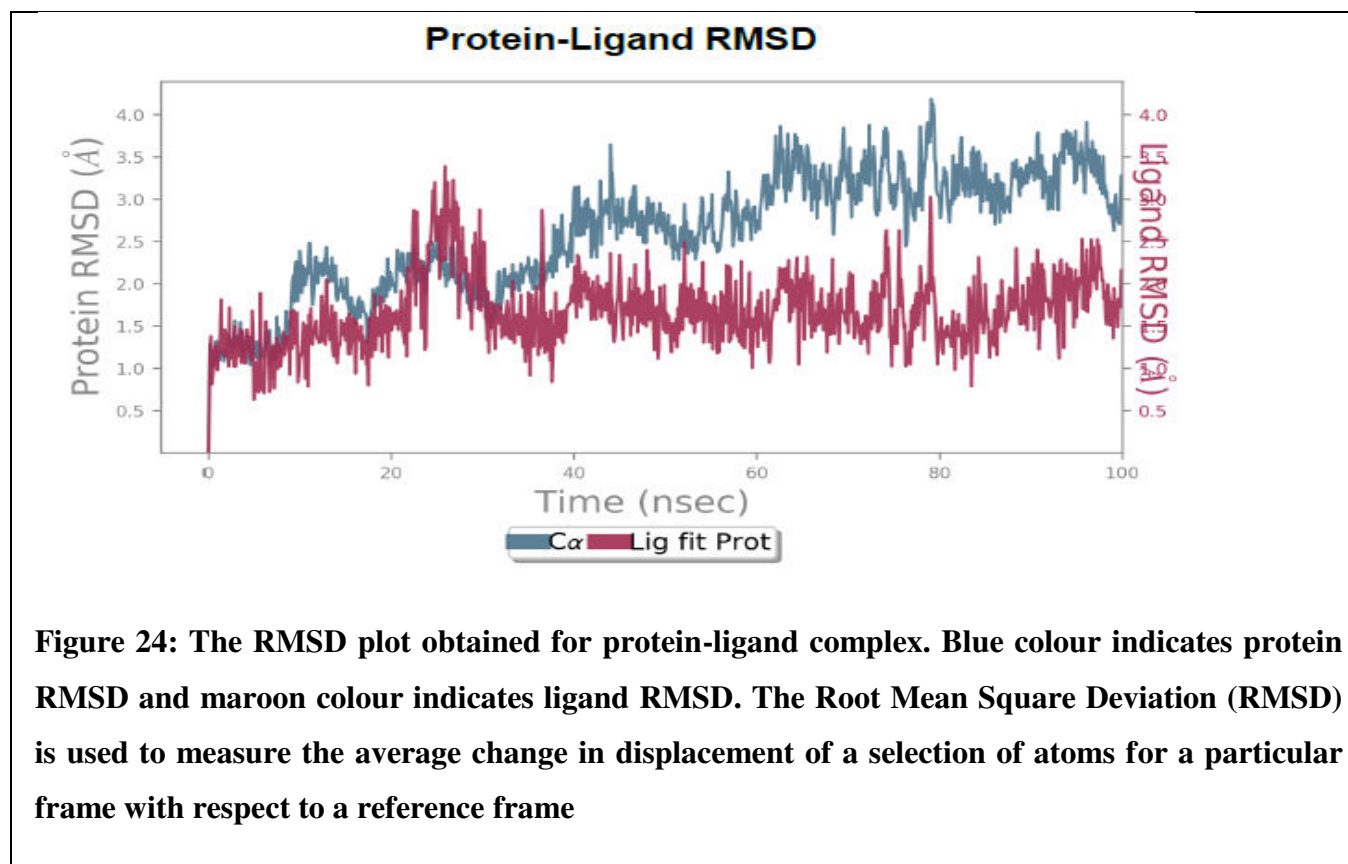
Protein RMSD:

The plot shows the RMSD evolution of a protein (left Y-axis). For the protein RMSD how the C-alpha and side chain RMSD evolved over 100ns period. All protein frames are first aligned on the reference frame backbone, and then the RMSD is calculated based on the atom selection, monitoring the RMSD of the protein can give insights into its structural conformation throughout the simulation. RMSD analysis can indicate if the simulation has equilibrated its fluctuations

towards the end of the simulation are around some thermal average structure. Changes of the order of 1-3 Å are perfectly acceptable for small, globular proteins. Changes much larger than that, however, indicate that the protein is undergoing a large conformational change during the simulation. It is also important that your simulation converges or that the RMSD values stabilize around a fixed value. If the RMSD of the protein is still increasing or decreasing on average at the end of the simulation, then the simulation may be too short so a longer simulation is required.

Ligand RMSD: Ligand RMSD (right Y-axis) indicates how stable the ligand is with respect to the protein and its binding pocket. In the above plot, 'Lig fit Prot' shows the RMSD of a ligand when the protein-ligand complex is first aligned on the protein backbone of the reference and then the RMSD of the ligand heavy atoms is measured. If the values observed are significantly larger than the RMSD of the protein, then it is likely that the ligand has diffused away from its initial binding site.

5-Methoxy-2-methyl-3-(4 (trifluoromethyl)benzylamino) naphthalene1,4-dione has better PL-RMSD value in the range 0.5-3.5Å throughout the simulation. The RMSD plot in indicated that the compound-**5-Methoxy-2-methyl-3-(4 (trifluoromethyl)benzylamino) naphthalene1,4-dione -3OY1** complex reached its stable form at 100ns. PL-RMSD shown in **(Figure 24)**



PL-Contacts: Protein interactions with the ligand can be monitored throughout the simulation. These interactions can be categorized by type and summarized, as shown in the Figure13. Protein-ligand interactions (or 'contacts') are categorized into four types: Hydrogen Bonds, Hydrophobic, Water Bridge and Ionic interactions. Each interaction type contains more specific subtypes, which can be explored through the 'Simulation Interactions Diagram' panel. The stacked bar charts are normalized over the course of the trajectory.

Hydrogen bonds play a significant role in ligand binding. Consideration of hydrogen-bonding properties in drug design is important because of their strong influence on drug specificity, metabolization and adsorption. Hydrophobic contacts generally these type of interactions involve a hydrophobic amino acid and an aromatic or aliphatic group on the ligand, but we have extended this category to also include pi-Cation interactions. Water Bridges: are hydrogen-bonded protein-ligand interactions mediated by a water molecule. The hydrogen-bond geometry is slightly relaxed from the standard H-bond definition.

The histogram displayed favored hydrophobic interactions with ILE70, VAL78, MET 146, ILE 124 and water bridge interactions with SER72, ASN151, and SER193. Hydrogen bond interaction was observed with MET149. The histogram chart was shown in **(Figure: 25)**.

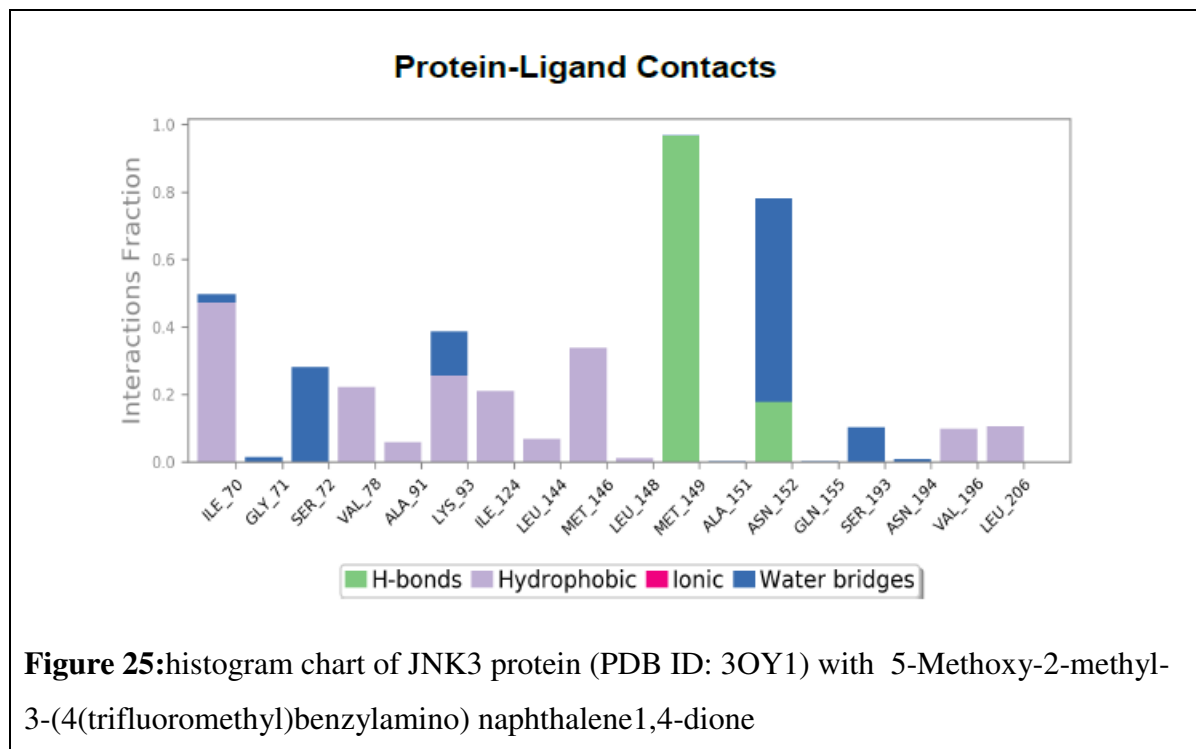
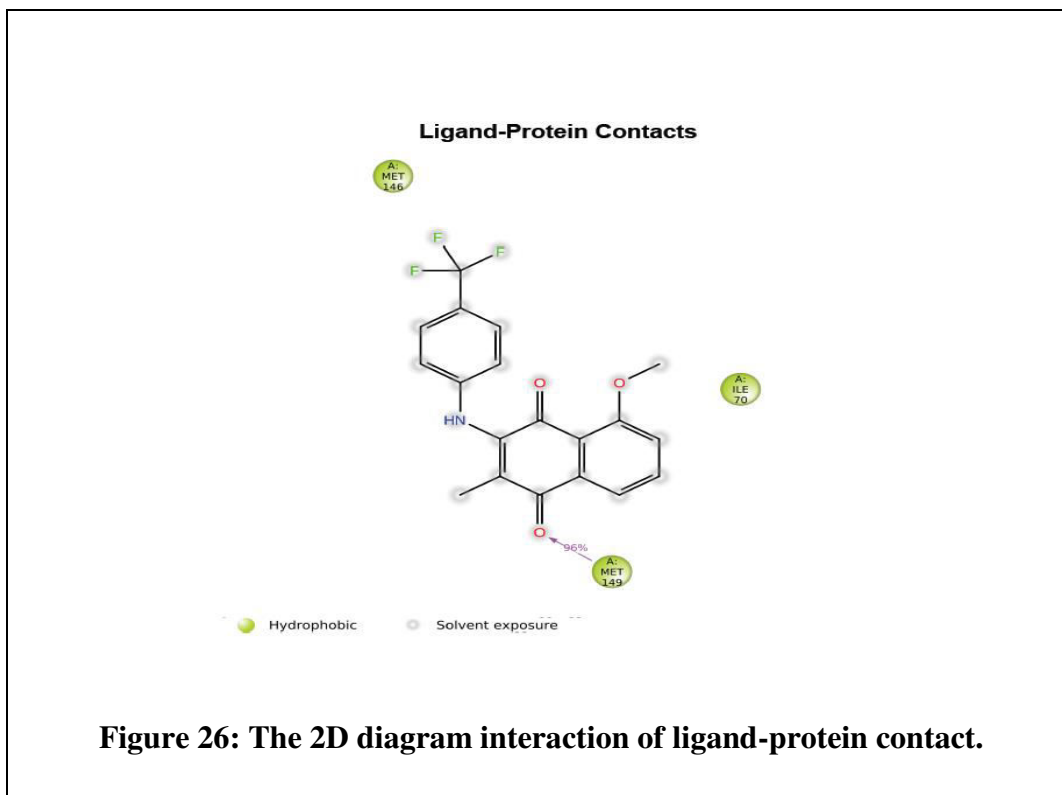


Figure 25: histogram chart of JNK3 protein (PDB ID: 3OY1) with 5-Methoxy-2-methyl-3-(4(trifluoromethyl)benzylamino) naphthalene 1,4-dione

L-P Contacts:

Figure 26: A schematic of detailed ligand atom interactions with the protein residues. Interactions that occur more than **30.0%** of the simulation time in the selected trajectory (0.00 through 100.00 nsec). The residue interactions were similar to docking results. LP-contacts displayed MET149 donate side chain hydrogen bond more than 90 percent of the time to this oxygen in the binding pocket of 3OY1.



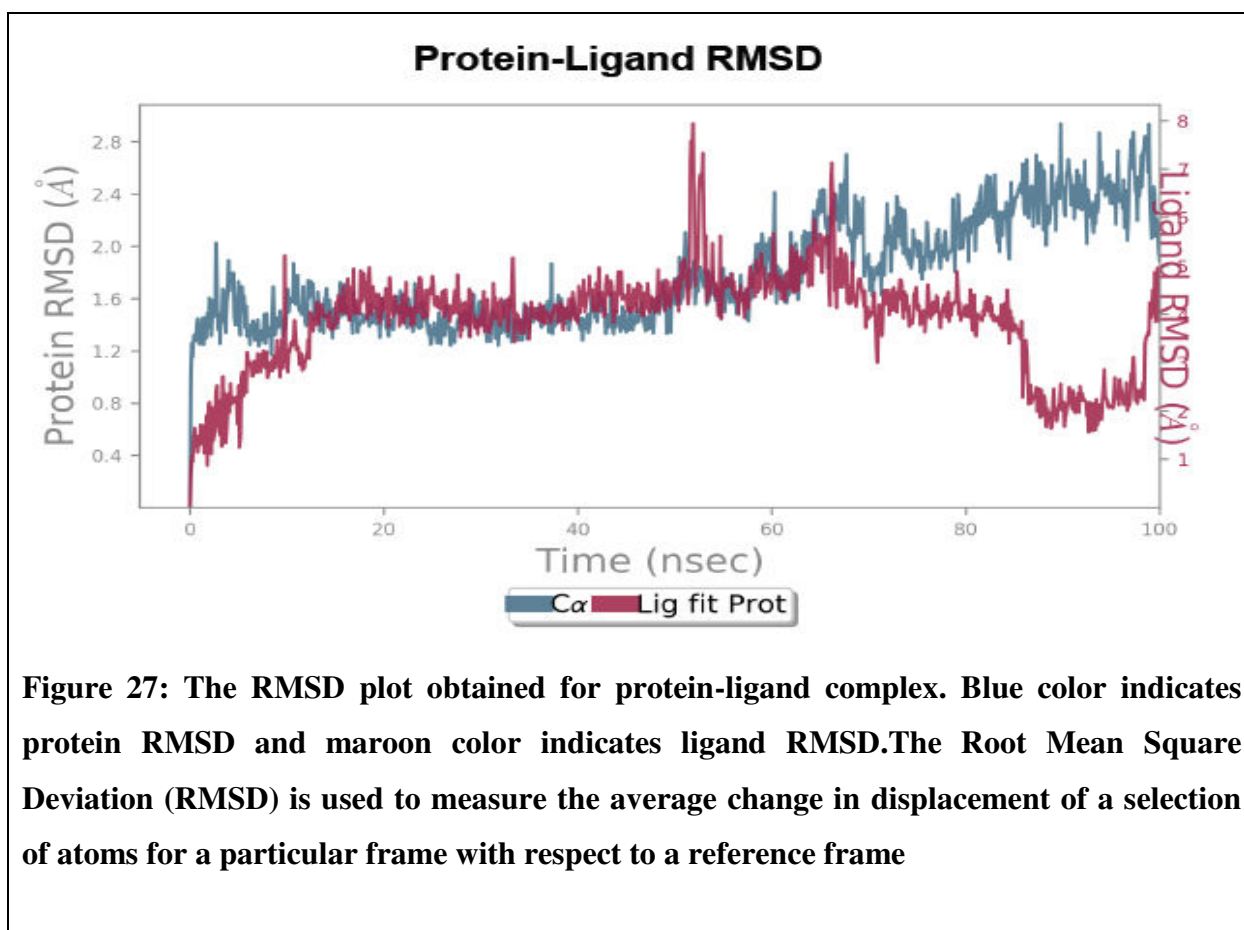
MD simulation of Shikonin with target JNK3 protein:

Protein RMSD:

The plot shows the RMSD evolution of a protein (left Y-axis). All protein frames are first aligned on the reference frame backbone, and then the RMSD is calculated based on the atom selection, monitoring the RMSD of the protein can give insights into its structural conformation throughout the simulation. RMSD analysis can indicate if the simulation has equilibrated its fluctuations towards the end of the simulation are around some thermal average structure. Changes of the order of 1-3 Å are perfectly acceptable for small, globular proteins. Changes much larger than that, however, indicate that the protein is undergoing a large conformational change during the simulation. It is also important that your simulation converges the RMSD values stabilize around a fixed value. If the RMSD of the protein is still increasing or decreasing on average at the end of the simulation, then your system has not equilibrated, and your simulation may not be long enough for rigorous analysis.

Ligand RMSD: Ligand RMSD (right Y-axis) indicates how stable the ligand is with respect to the protein and its binding pocket. In the above plot, 'Lig fit Prot' shows the RMSD of a ligand when the protein-ligand complex is first aligned on the protein backbone of the reference and then the RMSD of the ligand heavy atoms is measured. If the values observed are significantly larger than the RMSD of the protein, then it is likely that the ligand has diffused away from its initial binding site.

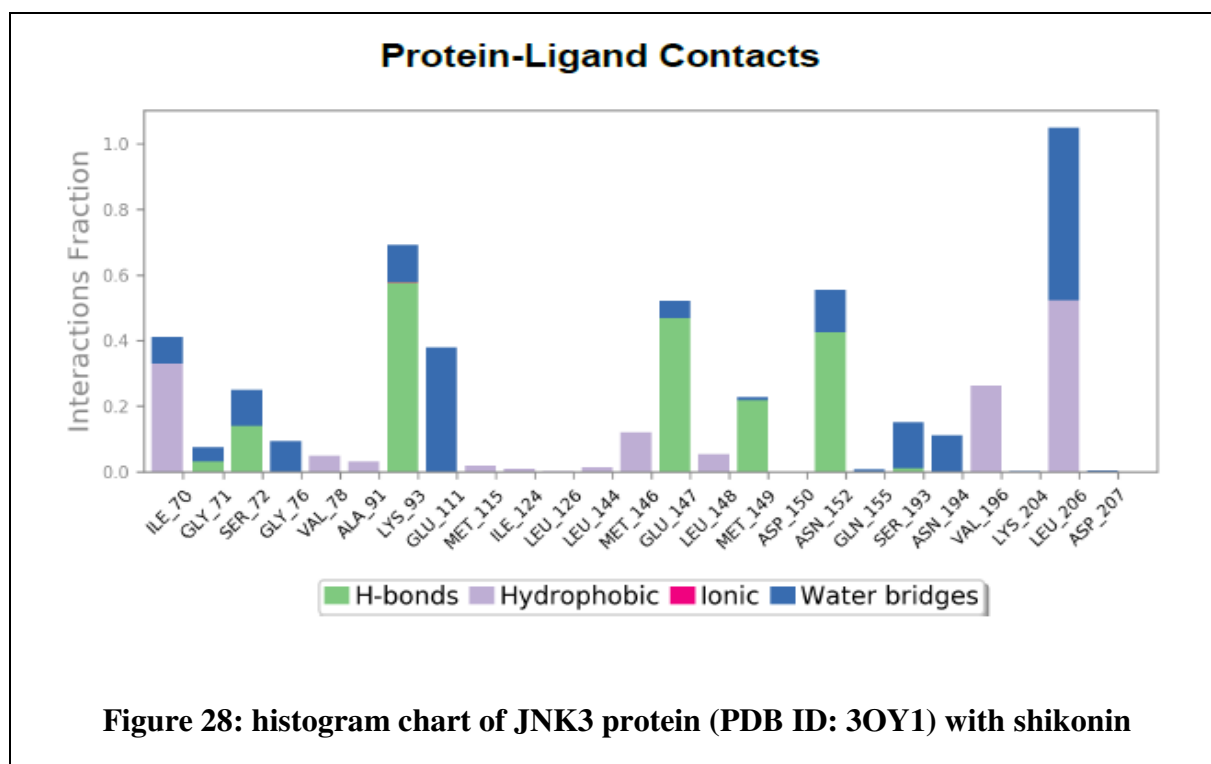
Shikonin has better PL-RMSD value in the range 0.4- 6Å throughout the simulation. The RMSD plot in indicated that the compound- **Shikonin-3OY1** complex reached its stable form at 100ns. PL-RMSD shown in (Figure 27)



PL-Contacts: Protein interactions with the ligand can be monitored throughout the simulation. These interactions can be categorized by type and summarized, as shown in the Figure13. Protein-ligand interactions (or 'contacts') are categorized into four types: Hydrogen Bonds,

Hydrophobic, Water Bridge and Ionic interactions. Each interaction type contains more specific subtypes, which can be explored through the 'Simulation Interactions Diagram' panel. The stacked bar charts are normalized over the course of the trajectory. Hydrogen bonds play a significant role in ligand binding. Consideration of hydrogen-bonding properties in drug design is important because of their strong influence on drug specificity, metabolism and adsorption. Hydrophobic contacts generally these type of interactions involve a hydrophobic amino acid and an aromatic or aliphatic group on the ligand, but we have extended this category to also include pi-Cation interactions. Water Bridges: are hydrogen-bonded protein-ligand interactions mediated by a water molecule. The hydrogen-bond geometry is slightly relaxed from the standard H-bond definition.

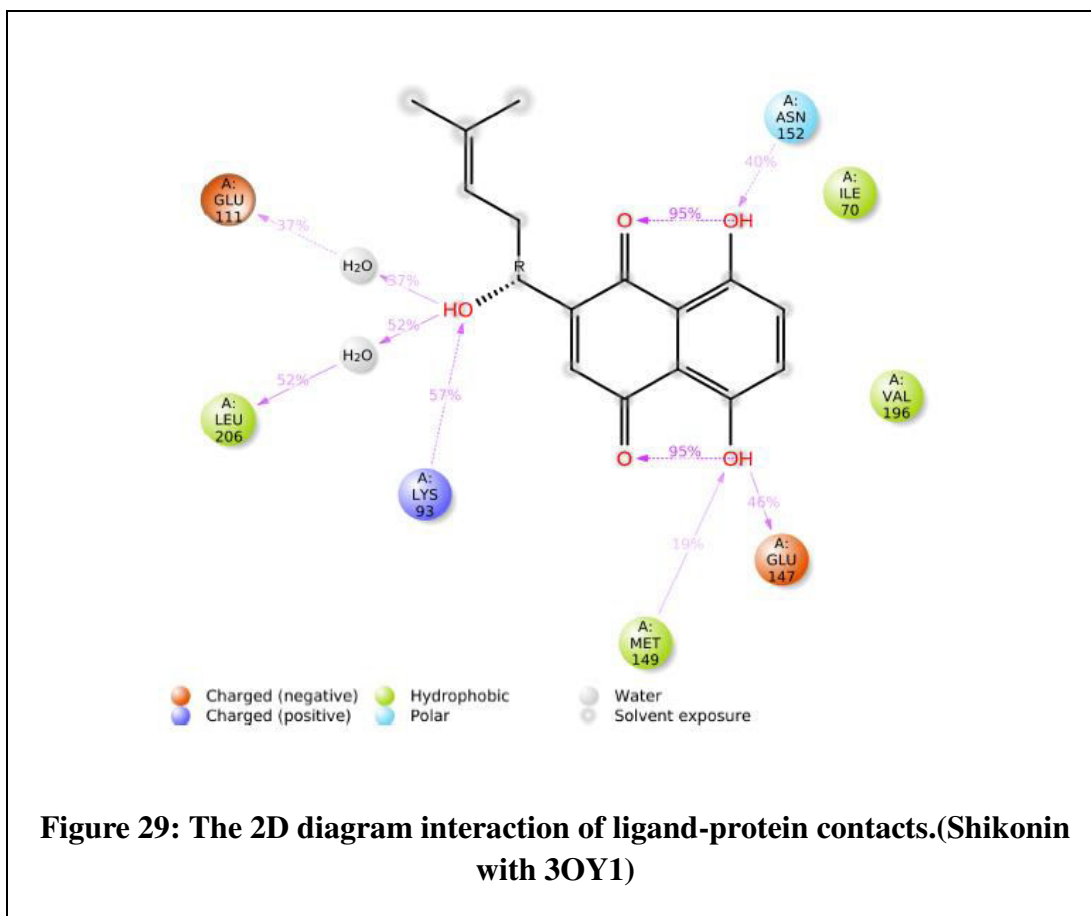
The histogram chart displayed favored hydrophobic interactions with ILE70, MET146, VAL196, LEU206, hydrogen bond interaction LYS93, GLU147, MET149, ASN152 and water bridge interactions with GLU111, SER193, and ASN194. The histogram charts are shown in **(Figure: 28)**.



L-P contacts:

Figure 29: A schematic of detailed ligand atom interactions with the protein residues. Interactions that occur more than **30.0%** of the simulation time in the selected trajectory (0.00 through 100.00 nsec)

Shikonin has hydroxyl group at side chain. The residue interactions were similar to docking results. Hydroxyl group at side chain displayed water bridged interaction with two amino acids GLU111 with 37%, LEU206 with 52% and also observed H-bond interaction with LYS93 (57%) respectively. Hydroxyl group at 8th position displayed hydrogen bond interaction with ASN152- (40%) and 5th position of hydroxyl group displayed H-bond interaction with GLU147 (46%), the lower the contact strength H-bond interaction observed with MET149 (19%) in the binding pocket of 3OY1.



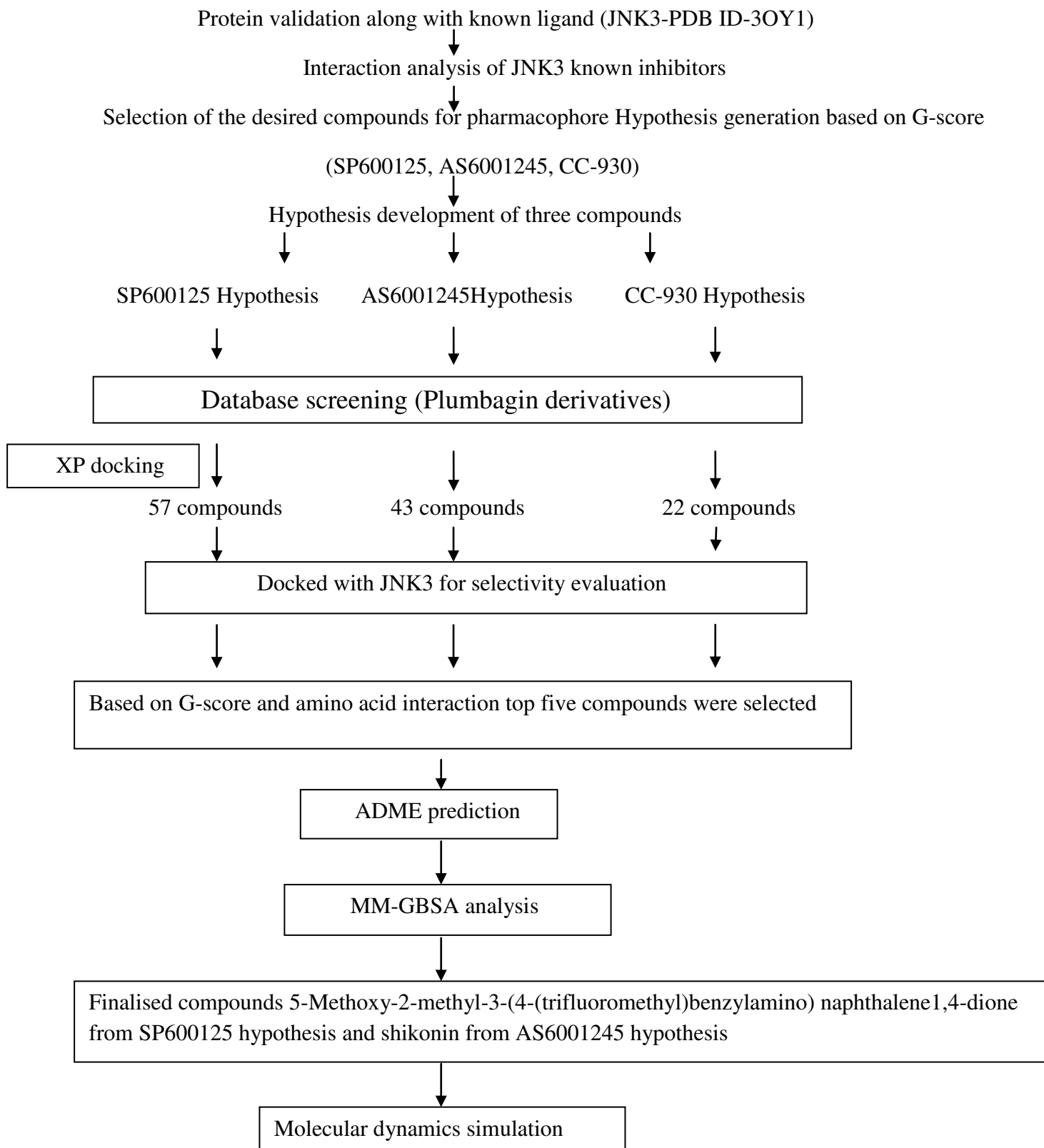


Figure 30: Schematic illustration of the overall workflow

Discussion

7. DISCUSSION

JNK signaling pathway is a cell death pathway that controls apoptosis signaling. The JNK pathway plays a pivotal role in cell death of several cell types and the activation of JNK3 appears to be essential for the pathophysiology of many neurodegenerative diseases (**Yamamoto et al., 2021**)

Several molecules with high specificity for JNK3 are currently in development, such as Quinazoline, Triazolothione, and a number of Pyridopyrimidinone derivatives in particular might be promising molecules in preventing neurodegeneration. They have shown good brain penetration and pharmacokinetic properties (**Cobos et al., 2022**)

The structure of JNK3 is composed of two lobes: a smaller N-terminal lobe with β strands and a larger helical C-terminal lobe. A flexible hinge-like region is connecting the two lobes. The ATP-binding site is located in a deep cleft at the junction of the N and C lobes. Most drug discovery efforts for JNKs have targeted this highly conserved ATP-binding region(**Nguyen et al., 2021**).several JNK3 inhibitors are shown to restore anti-oxidant enzyme activity and reduce the levels of oxidative stress-induced phosphorylation of JNK and neuroinflammatory mediators (**Zulfiqar et al., 2020**)

One of the first molecules to be investigated was SP600125 (PubChem ID 8515), a pan-JNK inhibitor with IC₅₀ values for JNK1, JNK2, and JNK3 of 40, 40, and 90 nM, respectively. previous studies showed that intracerebroventricular injections of SP600125 improved AD-related neurological aspects in animal models. SP600125 helped in understanding the role of JNK in many physiological and pathological conditions. Tanzisertib (Celgene) (PubChem ID 11597537) is a pan-JNK inhibitor developed based on the SP600125 structure with reported inhibition of JNK3 activity. Tanzisertib also known as CC-930, the safety of CC-930, an antifibrotic inhibitor of JNK was recently tested in phase II clinical trials. (**Messoussi et al., 2014**) Another SP600125 derivative that has been developed is CC-401 the compound entered a phase I clinical trial to determine the optimal dosing for individuals with high-risk myeloid leukemia, but the trial was discontinued. PG5001(bentamapimod and AS601245) is an another orally active ATP-competitive JNK inhibitor with an IC₅₀ of 80 nM, 90 nM, and 230 nM for JNK1, JNK2, and JNK3, respectively, Based on promising preliminary studies in animal models

of autoimmune diseases and neuronal apoptosis, PGL5001 was first described to have therapeutic potential in multiple sclerosis and fibrosis. PGL5001 is proposed as a potential first-in-class product for the treatment of endometriosis and is currently being evaluated in a Phase 2 clinical trial. (Palmer et al., 2016) (Hepp Rehfeldt et al., 2020),

(Joon-Hong et al., 2021) JNK inhibitors SP600125, AS601245 and CC-930 have been introduced and suggested to target JNK3 in neurodegenerative disease and also showing promising results in several invitro and invivo studies. SP600125, AS601245 blocks JNK3 with greater potency than JNK1 and JNK2. All three JNK isoforms have an ATP binding pocket with a highly conserved sequence. (Youri et al., 2020) Thus, few compounds exhibiting high selectivity for JNK3 have been discovered.

In the development process of JNK3 inhibitors, although JNK3 inhibitors have been researched for many years, only few drug candidates reached clinical trials, none of them was approved (Le fu et al., 2021)

The redocking results, we found that co-crystallized ligand also form the same hydrogen bonds interaction with MET149. Even the related literature has reported the effect of these hydrogen bond interactions on the inhibition. Therefore, the hydrogen bonds will be important evaluation criteria in evaluating the interaction between newly designed compounds and target proteins.

The pharmacophore modelling approaches have been an essential part of many drug discovery strategies. e-pharmacophore screening is viewed as a favourable approach in drug discovery to find a new inhibitor based on the ligand's stereo-electronic characteristics and their interactive interaction with biological receptors. Evaluated two point, three point and four point e-pharmacophore incorporated into pharmacophore based database screening from the phase module. Molecular docking is a very advanced and quick method to generate the various binding poses of ligand interaction in the active site with higher binding affinities. Docking study was conducted to understand the binding mode of the novel JNK3 inhibitors. When we performed the docking experiment of database compounds of plumbagin derivatives with a JNK3 protein (3OY1), we observed many interactions that could contribute to complex stabilization. The hinge binder formed one hydrogen bonds interaction with Met149 of JNK3 and the hydrophobic interactions formed with residues of Met146, Val79, Val145, Leu144, Ala91, Ile92, Ile124, and

Leu128. All hydrogen bond interaction showed hydrogen bond length below 2.2Å. All the compounds showed a dock score in the range 7.7-10.6. 5-Methoxy-2-methyl-3-(4(trifluoromethyl) benzylamino) naphthalene1,4-dione and shikonin showed highest dock score and similar amino acid interaction compared to others and reference compounds. Prediction ADME can be helpful in increasing the success rate and reducing the risk of failure in subsequent stage of drug development. Lipinski rule of five predicts the drug-like properties of chosen ligands. According to rule of five, a good drug should possess molecular weight less than 500, donor HB less than or equal to 5, acceptHB less than or equal to 10, and octanol/water partition coefficient (QPlogPo/w) less than or equal to 5. Compounds satisfying all these properties could be considered drug like. Bioavailability is described by the process of drug absorption and liver first-pass metabolism. Absorption is defined by transport of drug from the site of application to blood stream. Low availability is the common problem of many oral form of drugs due to poor solubility and slow absorption. Hence absorption greatly depends on solubility and permeability of the drug (Muthiah et al., 2021). Qikprop module was used to analyze ADME properties. The pharmacokinetic properties selected compounds are within the acceptable range likely having drug-like nature for human use. Binding affinity was estimated from the Glide score and the result was compared with standard drugs. Highest binding free energy of the compounds defines a greater affinity for binding to receptor. 5-Methoxy-2-methyl-3-(4(trifluoromethyl) benzylamino) naphthalene1,4-dione and shikonin have the highest binding free energy in the negative range -35.42 kcal/mol and -32.13 kcal/mol compared to the reference compounds. Various structural information with conformational behaviors of the protein in the presence of a ligand at atomic level can be investigated using a molecular dynamics simulation approach. Simulation studies provide a detailed explanation of stability characteristics and dynamic activities between a protein and a ligand. In molecular dynamics simulation, the interaction and the stability of the protein–ligand complex were calculated. MD simulation was carried out two best docking score compounds with target JNK3. The molecular docking and molecular dynamics results implied that relevant hydrogen interactions were very important for ligand-receptor binding, even which of them had been confirmed by the literature. The tested molecule shows H-bond interactions with the important amino acid MET149 similar to the reference compound, which is necessary for the inhibition of JNK3 in both docking and dynamic studies.

Conclusion

8. CONCLUSION

In the present work, rational approach combining e- pharmacophore modelling and structure-based virtual screening was employed on the target JNK3 to identify potential JNK3 inhibitors. The pharmacophore-based approaches are well known for their strength to propose a diverse set of molecules having diverse molecular frameworks but owing to a desired biological activity for one target. The hits were further analyzed and ranked by using dock score, binding energy, ADME parameters and MD simulations. Plumbagin derivatives have shown good potential of binding with the targeted protein as indicated by ΔG_{bind} score. They also possessed desired ADME properties. Thereafter, MD simulation studies were carried out two best docked complexes. Based on the key amino acid residues interactions, molecular dynamics simulation indicates that the docked complex of **5-Methoxy-2-methyl-3(4(trifluoromethyl)benzylamino) naphthalene1, 4-dione and shikonin** with JNK3 protein (3OY1) have a good stability in the binding pocket. The significant interaction with residue MET 149 was observed in both molecular docking and molecular dynamics simulations studies. By confirm the binding affinities of the ligand and the accurate interactions, molecular dynamics simulations valid the results of molecular docking. The results showed that the best classified compounds 5-Methoxy-2-methyl-3-(4(trifluoromethyl)benzylamino) naphthalene1, 4-dione and shikonin with highest docking score and binding affinity and stable hydrogen bond with MET149 and hydrophobic interactions with Met146, Val79, Val145, Leu144, Ala91, Ile92, Ile124, and Leu128. relative to reference compounds. The outcome reveal that this study provides evidence for the consideration of plumbagin derivatives as potential JNK3 inhibitors. Therefore, reliable computer-aided drug design methods could play an increasingly important role in the future drug discovery process. The *Insilico* studies results revealed that **5-Methoxy-2-methyl-3-(4 (trifluoromethyl) benzylamino) naphthalene1,4-dione and Shikonin** as a potent, selective JNK3 inhibitors. This was found out by screening of generated pharmacophore hypothesis, molecular docking and molecular dynamics study of plumbagin and its derivatives. Further, *in vitro* evaluation of 5-Methoxy-2-methyl-3-(4-(trifluoromethyl) benzylamino) naphthalene1,4-dione and Shikonin is the futuristic requirement in order to perceive additional activity validation.

References

9. REFERENCES

1. Akhilraj AR, Bhat S, Priyalatha B, Vimala KS. Comparative hepatoprotective activity of detoxified roots of *Plumbago zeylanica* L. and *Plumbago rosea* L. in Wistar rats. *Journal of Ayurveda and Integrative Medicine*. 2021 Jul 1;12(3):452-7
2. Braithwaite SP, Schmid RS, He DN, Sung ML, Cho S, Resnick L, Monaghan MM, Hirst WD, Essrich C, Reinhart PH, Lo DC. Inhibition of c-Jun kinase provides neuroprotection in a model of Alzheimer's disease. *Neurobiology of disease*. 2010 Sep 1; 39(3):311-7.
3. Brandalise F, Cesaroni V, Gregori A, Repetti M, Romano C, Orrù G, Botta L, Girometta C, Guglielminetti ML, Savino E, Rossi P. Dietary supplementation of *Hericium erinaceus* increases mossy fiber-CA3 hippocampal neurotransmission and recognition memory in wild-type mice. *Evidence-Based Complementary and Alternative Medicine*. 2017 Jan 1;2017
4. Campora M, Francesconi V, Schenone S, Tasso B, Tonelli M. Journey on Naphthoquinone and Anthraquinone Derivatives: New Insights in Alzheimer's Disease. *Pharmaceuticals*. 2021 Jan;14(1):33.
5. Checker R, Patwardhan RS, Sharma D, Sandur SK. Chemopreventive and anticancer effects of plumbagin: Novel mechanism (s) via modulation of cellular redox. In *Role of Nutraceuticals in Cancer Chemosensitization 2018* Jan 1 (pp. 325-341). Academic Press.
6. Chen X, Jiang H. Tau as a potential therapeutic target for ischemic stroke. *Aging (Albany NY)*. 2019 Dec 31;11(24):12827.
7. Chen Y, Zheng X, Wang Y, Song J. Effect of PI3K/Akt/mTOR signaling pathway on JNK3 in Parkinsonian rats. *Experimental and therapeutic medicine*. 2019 Mar 1;17(3):1771-5.
8. Cobos SN, Torrente MP. Epidrugs in Amyotrophic Lateral Sclerosis/Frontotemporal Dementia: Contextualizing a Role for Histone Kinase Inhibition in Neurodegenerative Disease. *ACS Pharmacology & Translational Science*. 2022 Jan 21.
9. Darusman F, Fakhri TM. Comprehensive InSilico Analysis of Christinin Molecular Behaviour from *Ziziphusspina-christi* Leaves on *Propionibacterium acnes*. *Pharmaceutical Sciences and Research*. 2021; 8(1):5.
10. Dhanasekaran DN, Reddy EP. JNK signaling in apoptosis. *Oncogene*. 2008 Oct; 27(48):6245-51.

11. Dhingra D, Bansal S. Antidepressant-like activity of plumbagin in unstressed and stressed mice. *Pharmacological Reports*. 2015 Oct 1; 67(5):1024-32.
12. Dickens M, Rogers JS, Cavanagh J, Raitano A, Xia Z, Halpern JR, Greenberg ME, Sawyers CL, Davis RJ. A cytoplasmic inhibitor of the JNK signal transduction pathway. *Science*. 1997 Aug 1; 277(5326):693-6.
13. El Aissouq A, Toufik H, Stitou M, Ouammou A, Lamchouri F. In silico design of novel tetra-substituted pyridinylimidazoles derivatives as c-jun N-terminal kinase-3 inhibitors, using 2D/3D-QSAR studies, molecular docking and ADMET prediction. *International Journal of Peptide Research and Therapeutics*. 2020 Sep;26(3):1335-51
14. Eminel S, Roemer L, Waetzig V, Herdegen T. c-Jun N-terminal kinases trigger both degeneration and neurite outgrowth in primary hippocampal and cortical neurons. *Journal of neurochemistry*. 2008 Feb;104(4):957-69.
15. Fu L, Chen Y, Guo HM, Xu L, Tan MN, Dong Y, Shu M, Wang R, Lin ZH. A selectivity study of polysubstituted pyridinylimidazoles as dual inhibitors of JNK3 and p38 α MAPK based on 3D-QSAR, molecular docking, and molecular dynamics simulation. *Structural Chemistry*. 2021 Apr;32(2):819-34
16. Hazra B, Sarkar R, Bhattacharyya S, Ghosh PK, Chel G, Dinda B. Synthesis of plumbagin derivatives and their inhibitory activities against Ehrlich ascites carcinoma in vivo and *Leishmania donovani* promastigotes in vitro. *Phytotherapy Research: An International Journal Devoted to Pharmacological and Toxicological Evaluation of Natural Product Derivatives*. 2002 Mar; 16(2):133-7.
17. Hazra B, Sarma MD, Sanyal U. Separation methods of quinonoid constituents of plants used in Oriental traditional medicines. *Journal of Chromatography B*. 2004 Dec 5;812(1-259-75).
18. Hepp Rehfeldt SC, Majolo F, Goettert MI, Laufer S. c-Jun N-terminal kinase inhibitors as potential leads for new therapeutics for Alzheimer's diseases. *International journal of molecular sciences*. 2020 Jan;21(24):9677
19. Huang XL, Liu C, Shi XM, Cheng YT, Zhou Q, Li JP, Liao J. Zoledronic acid inhibits osteoclastogenesis and bone resorptive function by suppressing RANKL-mediated NF- κ B and JNK and their downstream signalling pathways. *Molecular Medicine Reports*. 2022 Feb 1;25(2):1-2.

-
20. James JP, FabinAM, Sasidharan P, Kumar P. Virtual Screening, Molecular Docking and Pharmacophore Modeling of Phytoconstituents of Flavones as Aldose Reductase Inhibitors.2021
 21. Jang M, Oh Y, Cho H, Yang S, Moon H, Im D, Hah JM. Discovery of 1-Pyrimidinyl-2-Aryl-4, 6-Dihydropyrrolo [3, 4-d] Imidazole-5 (1H)-Carboxamide as a Novel JNK Inhibitor. *International journal of molecular sciences*. 2020 Jan;21(5):1698.
 22. Jangra A, Chadha V, Kumar D, Kumar V, Arora MK. Neuroprotective and acetylcholinesterase inhibitory activity of plumbagin in ICV-LPS induced behavioral deficits in rats. *Current Research in Behavioral Sciences*. 2021 Nov 1;2:100060.
 23. Jing LI, Anning LI. Role of JNK activation in apoptosis: a double-edged sword. *Cell research*. 2005 Jan;15(1):36-42.
 24. Johnson GL, Nakamura K. The c-jun kinase/stress-activated pathway: regulation, function and role in human disease. *BiochimicaetBiophysicaActa (BBA)-Molecular Cell Research*. 2007 Aug 1; 1773(8):1341-8.
 25. Jun JH, Baek JH, Yang SY, Moon HW, Kim HJ, Cho HW, Hah JM. Discovery of a Potent and Selective JNK3 Inhibitor with Neuroprotective Effect against Amyloid β -Induced Neurotoxicity in Primary Rat Neurons. *International journal of molecular sciences*. 2021 Jan; 22(20):11084.
 26. Jung H, Aman W, Hah JM. Novel scaffold evolution through combinatorial 3D-QSAR model studies of two types of JNK3 inhibitors. *Bioorganic & medicinal chemistry letters*. 2017 May 15;27(10):2139-43.
 27. Kalirajan R, Pandiselvi A, Gowramma B, Balachandran P. In-silico design, ADMET screening, MM-GBSA binding free energy of some novel isoxazole substituted 9-anilinoacridines as HER2 inhibitors targeting breast cancer. *Current Drug Research Reviews Formerly: Current Drug Abuse Reviews*. 2019 Dec 1;11(2):118-28.
 28. Kumar A, Rathi E, Kini SG. E-pharmacophoremodelling, virtual screening, molecular dynamics simulations and in-silico ADME analysis for identification of potential E6 inhibitors against cervical cancer. *Journal of Molecular Structure*. 2019 Aug 5; 1189:299-306.omics, in silico toxicity, in vitro and in vivo studies. *Computers in Biology and Medicine*. 2021 May 2:104462.

-
29. Kumar GP, Khanum F. Neuroprotective potential of phytochemicals. *Pharmacognosy reviews*. 2012 Jul;6(12):81.
 30. Lange A, Günther M, Büttner FM, Zimmermann MO, Heidrich J, Hennig S, Zahn S, Schall C, Sievers-Engler A, Ansideri F, Koch P. Targeting the gatekeeper MET146 of C-Jun N-terminal kinase 3 induces a bivalent halogen/chalcogen bond. *Journal of the American Chemical Society*. 2015 Nov 25; 137(46):14640-52.
 31. Lee HP, Chen PC, Wang SW, Fong YC, Tsai CH, Tsai FJ, Chung JG, Huang CY, Yang JS, Hsu YM, Li TM. Plumbagin suppresses endothelial progenitor cell-related angiogenesis in vitro and in vivo. *Journal of Functional Foods*. 2019 Jan 1; 52:537-44.
 32. Long J, Cai L, Li J, Zhang L, Yang H, Wang T. JNK3 involvement in nerve cell apoptosis and neurofunctional recovery after traumatic brain injury. *Neural regeneration research*. 2013 Jun 5;8(16):1491.
 33. Luo P, Wong YF, Ge L, Zhang ZF, Liu Y, Liu L, Zhou H. Anti-inflammatory and analgesic effect of plumbagin through inhibition of nuclear factor- κ B activation. *Journal of Pharmacology and Experimental Therapeutics*. 2010 Dec 1; 335(3):735-42.
 34. Mehan S, Meena H, Sharma D, Sankhla R. JNK: a stress-activated protein kinase therapeutic strategies and involvement in Alzheimer's and various neurodegenerative abnormalities. *Journal of Molecular Neuroscience*. 2011 Mar; 43(3):376-90.
 35. Messoussi A, Feneyrolles C, Bros A, Deroide A, Daydé-Cazals B, Chev e G, Van Hijfte N, Fauvel B, Bougrin K, Yasri A. Recent progress in the design, study, and development of c-Jun N-terminal kinase inhibitors as anticancer agents. *Chemistry & biology*. 2014 Nov 20;21(11):1433-43.
 36. Morel C, Standen CL, Jung DY, Gray S, Ong H, Flavell RA, Kim JK, Davis RJ. Requirement of JIP1-mediated c-Jun N-terminal kinase activation for obesity-induced insulin resistance. *Molecular and Cellular Biology*. 2010 Oct 1; 30(19):4616-25.
 37. Musi CA, Agr o G, Santarella F, Iervasi E, Borsello T. JNK3 as therapeutic target and biomarker in neurodegenerative and neurodevelopmental brain diseases. *Cells*. 2020 Oct;9(10):2190.
 38. Nakhate KT, Bharne AP, Verma VS, Aru DN, Kokare DM. Plumbagin ameliorates memory dysfunction in streptozotocin induced Alzheimer's disease via activation of

-
- Nrf2/ARE pathway and inhibition of β -secretase. *Biomedicine & Pharmacotherapy*. 2018 May 1;101:379-90.
39. Nguyen PL, Bui BP, Duong MT, Lee K, Ahn HC, Cho J. Suppression of LPS-Induced Inflammation and Cell Migration by Azelastine through Inhibition of JNK/NF- κ B Pathway in BV2 Microglial Cells. *International Journal of Molecular Sciences*. 2021 Jan;22(16):9061.
40. O'Brien RJ, Wong PC. Amyloid precursor protein processing and Alzheimer's disease. *Annual review of neuroscience*. 2011 Jul 21;34:185-204.
41. Oh Y, Jang M, Cho H, Yang S, Im D, Moon H, Hah JM. Discovery of 3-alkyl-5-aryl-1-pyrimidyl-1 H-pyrazole derivatives as a novel selective inhibitor scaffold of JNK3. *Journal of enzyme inhibition and medicinal chemistry*. 2020 Jan 1; 35(1):372-6.
42. Palmer SS, Altan M, Denis D, Tos EG, Gotteland JP, Osteen KG, Bruner-Tran KL, Nataraja SG. Bentamapimod (JNK inhibitor AS602801) induces regression of endometriotic lesions in animal models. *Reproductive Sciences*. 2016 Jan;23(1):11-23.
43. Panwar U, Singh SK. Atom-based 3D-QSAR, molecular docking, DFT, and simulation studies of acylhydrazone, hydrazine, and diazene derivatives as IN-LEDGF/p75 inhibitors. *Structural Chemistry*. 2021 Feb;32(1):337-52.
44. Ploia C, Antoniou X, Scip A, Grande V, Cardinetti D, Colombo A, Canu N, Benussi L, Ghidoni R, Forloni G, Borsello T. JNK plays a key role in tau hyperphosphorylation in Alzheimer's disease models. *Journal of Alzheimer's disease*. 2011 Jan 1; 26(2):315-29.
45. Plotnikov MB, Chernysheva GA, Smolyakova VI, Aliev OI, Trofimova ES, Sherstoboev EY, Osipenko AN, Khlebnikov AI, Anfinogenova YJ, Schepetkin IA, Atochin DN. Neuroprotective effects of a novel inhibitor of c-Jun N-terminal kinase in the rat model of transient focal cerebral ischemia. *Cells*. 2020 Aug; 9(8):1860.
46. Rajalakshmi S, Vyawahare N, Pawar A, Mahaparale P, Chellampillai B. Current development in novel drug delivery systems of bioactive molecule plumbagin. *Artificial cells, nanomedicine, and biotechnology*. 2018 Oct 31; 46(sup1):209-18.
47. Sharma V, Kumar H, Wakode S. Pharmacophore generation and atom based 3D-QSAR of quinoline derivatives as selective phosphodiesterase 4B inhibitors. *RSC advances*. 2016;6(79):75805-19.

-
48. Shen Q, Liu L, Gu X, Xing D. Photobiomodulation suppresses JNK3 by activation of ERK/MKP7 to attenuate AMPA receptor endocytosis in Alzheimer's disease. *Aging cell*. 2021 Jan;20(1):e13289.
 49. Shi W, Fang Y, Jiang Y, Jiang S, Li Y, Li W, Xu M, Aschner M, Liu G. Plumbagin attenuates traumatic tracheal stenosis in rats and inhibits lung fibroblast proliferation and differentiation via TGF- β 1/Smad and Akt/mTOR pathways. *Bioengineered*. 2021 Jan 1;12(1):4475-88.
 50. ShridharDeshpande N, Mahendra GS, Aggarwal NN, Gatphoh BF, Revanasiddappa BC. Insilico design, ADMET screening, MM-GBSA binding free energy of novel 1, 3, 4 oxadiazoles linked Schiff bases as PARP-1 inhibitors targeting breast cancer. *Future Journal of Pharmaceutical Sciences*. 2021 Dec; 7(1):1-0.
 51. Singh A, Singh DK, Kharwar RN, White JF, Gond SK. Fungal endophytes as efficient sources of plant-derived bioactive compounds and their prospective applications in natural product drug discovery: Insights, avenues, and challenges. *Microorganisms*. 2021 Jan;9(1):197.
 52. Singh AK, Rana HK, Singh V, Yadav TC, Varadwaj P, Pandey AK. Evaluation of antidiabetic activity of dietary phenolic compound chlorogenic acid in streptozotocin induced diabetic rats: molecular docking, molecular dynamics.2021
 53. Singh N, Upadhyay S, Jaiswar A, Mishra N. In silico Docking Studies and Potential Lead Identification against JNK3 for Alzheimer's disease. *International Journal of Pharmaceutical Investigation*. 2019 Dec 12; 9(4):220-2.
 54. Singh P, Singh RK. Synthesis of Hydrazone Derivatives and In-silico docking studies against JNK protein to assess anticonvulsant activity of synthesized derivatives. *Journal of Pharmaceutical Sciences and Research*. 2020 Jun 1; 12(6):770-9.
 55. Solinas G, Vilcu C, Neels JG, Bandyopadhyay GK, Luo JL, Naugler W, Grivennikov S, Wynshaw-Boris A, Scadeng M, Olefsky JM, Karin M. JNK1 in hematopoietically derived cells contributes to diet-induced inflammation and insulin resistance without affecting obesity. *Cell metabolism*. 2007 Nov 7; 6(5):386-97.
 56. Son TG, Camandola S, Arumugam TV, Cutler RG, Telljohann RS, Mughal MR, Moore TA, Luo W, Yu QS, Johnson DA, Johnson JA. Plumbagin, a novel Nrf2/ARE activator, protects against cerebral ischemia. *Journal of neurochemistry*. 2010 Mar;112(5):1316-26

-
57. Syaifie PH, Hemasita AW, Nugroho DW, Mardiyati E, Anshori I. In Silico Investigation of Propolis Compounds as Potential Neuroprotective Agent.
 58. Tournier C, Dong C, Turner TK, Jones SN, Flavell RA, Davis RJ. MKK7 is an essential component of the JNK signal transduction pathway activated by proinflammatory cytokines. *Genes & development*. 2001 Jun 1; 15(11):1419-26.
 59. Wang CC, Chiang YM, Sung SC, Hsu YL, Chang JK, Kuo PL. Plumbagin induces cell cycle arrest and apoptosis through reactive oxygen species/c-Jun N-terminal kinase pathways in human melanoma A375. S2 cells. *Cancer letters*. 2008 Jan 18; 259(1):82-98.
 - Nadhan R, Patra D, Krishnan N, Rajan A, Gopala S, Ravi D, Srinivas P. Perspectives on mechanistic implications of ROS inducers for targeting viral infections. *European Journal of Pharmacology*. 2021 Jan 5;890:173621
 60. Wang S, Ren X, Hu X, Zhou L, Zhang C, Zhang M. Cadmium-induced apoptosis through reactive oxygen species-mediated mitochondrial oxidative stress and the JNK signaling pathway in TM3 cells, a model of mouse Leydig cells. *Toxicology and applied pharmacology*. 2019 Apr 1; 368:37-48.
 61. Wang W, Shi L, Xie Y, Ma C, Li W, Su X, Huang S, Chen R, Zhu Z, Mao Z, Han Y. SP600125, a new JNK inhibitor, protects dopaminergic neurons in the MPTP model of Parkinson's disease. *Neuroscience research*. 2004 Feb 1; 48(2):195-202.
 62. Wen XR, Fu YY, Liu HZ, Wu J, Shao XP, Zhang XB, Tang M, Shi Y, Ma K, Zhang F, Wang YW. Neuroprotection of sevoflurane against ischemia/reperfusion-induced brain injury through inhibiting JNK3/caspase-3 by enhancing Akt signaling pathway. *Molecular neurobiology*. 2016 Apr 1;53(3):1661-71
 63. Wu Q, Wu W, Jacevic V, Franca TC, and Wang X, Kuca K. Selective inhibitors for JNK signalling: a potential targeted therapy in cancer. *Journal of enzyme inhibition and medicinal chemistry*. 2020 Jan 1; 35(1):574-83.
 64. Wu Q, Wu W, Jacevic V, Franca TC, and Wang X, Kuca K. Selective inhibitors for JNK signalling: a potential targeted therapy in cancer. *Journal of enzyme inhibition and medicinal chemistry*. 2020 Jan 1;35(1):574-83.
 65. Xue D, Zhou X, Qiu J. Cytotoxicity mechanisms of plumbagin in drug-resistant tongue squamous cell carcinoma. *Journal of Pharmacy and Pharmacology*. 2021 Jan; 73(1):98-109.

66. Yamamoto S, Kayama T, Noguchi-Shinohara M, Hamaguchi T, Yamada M, Abe K, Kobayashi S. Rosmarinic acid suppresses tau phosphorylation and cognitive decline by downregulating the JNK signaling pathway. *NPJ science of food*. 2021 Jan 29;5(1):1-1.
67. Yarza R, Vela S, Solas M, Ramirez MJ. c-Jun N-terminal kinase (JNK) signaling as a therapeutic target for Alzheimer's disease. *Frontiers in pharmacology*. 2016 Jan 12; 6:321.
68. Yasuda J, Whitmarsh AJ, Cavanagh J, Sharma M, Davis RJ. The JIP group of mitogen-activated protein kinase scaffold proteins. *Molecular and cellular biology*. 1999 Oct 1;19(10):7245-54.
69. Yong R, Chen XM, Shen S, Vijayaraj S, Ma Q, Pollock CA, Saad S. Plumbagin ameliorates diabetic nephropathy via interruption of pathways that include NOX4 signalling. *PLoS One*. 2013 Aug 26;8(8):e73428.
70. Yuan JH, Pan F, Chen J, Chen CE, Xie DP, Jiang XZ, Guo SJ, Zhou J. Neuroprotection by plumbagin involves BDNF-TrkB-PI3K/Akt and ERK1/2/JNK pathways in isoflurane-induced neonatal rats. *Journal of Pharmacy and Pharmacology*. 2017 Jul;69(7):896-906.
71. Zhang G, Ni X, Zhou Y. Cardioprotective effect of plumbagin and amelioration of pro-inflammatory cytokines through suppression of Na⁺/K⁺-ATPase on myocardial ischemia. *Pharmacognosy Magazine*. 2021 Jul 1;17(75):643.
72. Zhang Q, Zhao S, Zheng W, Fu H, Wu T, Hu F. Plumbagin attenuated oxygen-glucose deprivation/reoxygenation-induced injury in human SH-SY5Y cells by inhibiting NOX4-derived ROS-activated NLRP3 inflammasome. *Bioscience, biotechnology, and biochemistry*. 2020 Jan 2;84(1):134-42.
73. Zhao Y, Kuca K, Wu W, Wang X, Nepovimova E, Musilek K, and Wu Q. Hypothesis: JNK signaling is a therapeutic target of neurodegenerative diseases. *Alzheimer's & Dementia*. 2021 May 25.
74. Zhao Y, Kuca K, Wu W, Wang X, Nepovimova E, Musilek K, and Wu Q. Hypothesis: JNK signaling is a therapeutic target of neurodegenerative diseases. *Alzheimer's & Dementia*. 2021 May 25.
75. Zulfiqar Z, Shah FA, Shafique S, Alattar A, Ali T, Alvi AM, Rashid S, Li S. Repurposing FDA Approved Drugs as JNK3 Inhibitor for Prevention of Neuroinflammation Induced by MCAO in Rats. *Journal of Inflammation Research*. 2020; 13:1185.

76. Zulfiqar Z, Shah FA, Shafique S, Alattar A, Ali T, Alvi AM, Rashid S, Li S. Repurposing FDA Approved Drugs as JNK3 Inhibitor for Prevention of Neuroinflammation Induced by MCAO in Rats. *Journal of Inflammation Research*. 2020; 13:1185.

Annexure



Certificate Of Participation

This is to certify that

Susmitha.P

has attended 3 days International e-Workshop on **“Docking, QSAR and Molecular Dynamics”** jointly organized by Department of Biotechnology, Ramaiah Institute of Technology and Department of Pharmaceutical Chemistry, Faculty of Pharmacy, Ramaiah University of Applied Sciences, Bengaluru, Karnataka, India in association with IEEE-EMB MSRT student chapter and SRIGEN-Society of Biotechnologists from 29 to 31 July 2020.

Dr. Bindu S
Professor and Head
Department of Biotechnology, RIT

Prof. C.H.S. Venkataramana
Professor and Head
Department of Pharmaceutical Chemistry
FPH, RUAS

Dr. V. Madhavan
Dean, FPH, RUAS



**MANIPAL COLLEGE
OF PHARMACEUTICAL SCIENCES**
MANIPAL
(A constituent unit of MAHE, Manipal)

National e-Conference on Drug Discovery for CNS Disorders

CERTIFICATE OF PARTICIPATION

This is to certify that

Ms. Susmitha Palaniyappan

has participated as a Delegate

in the National e-Conference on Drug Discovery for CNS Disorders held between 6 – 10 December 2021.

– Jointly organized by –

Department of Pharmacology, Manipal College of Pharmaceutical Sciences and Centre for Digital Learning, MAHE, Manipal, India

– Supported by –

Vision Group on Science and Technology (VGST), Karnataka Science and Technology Promotion Society (KSTePS),

Department of Electronics, Information Technology, Biotechnology & Science and Technology, Government of Karnataka, India

Dr. Anoop Kishore

Co-ordinator, Centre for Digital Learning
MAHE, Manipal

Dr. K Nandakumar

Head, Department of Pharmacology
MCOPS, MAHE, Manipal

Dr. C Mallikarjuna Rao

Convener, CNSCON-2021
Principal, MCOPS, MAHE, Manipal



Group Pharmaceuticals Ltd
healthy smiles matter

eppendorf

Lead
MoleQules

Triune

**Juniper[®]
Life
Sciences**

**SCIENTIFIC
ENTERPRISES**
ISO 9001:2015 CERTIFIED



The Organizing Committee of the
“International Conference on Medicinal and Food Plant Research & 3rd Sino-CPLP Symposium on
Natural Products and Biodiversity Resources”, 9-10th April 2021, Hanzhong, China

This is to confirm that

Susmitha Palaniyappan

*Attended the International Conference on Medicinal and Food Plant Research &
3rd Sino-CPLP Symposium on Natural Products and Biodiversity Resources*

Distinguished Professor at Shaanxi
University of Technology
Senior Researcher, CBMA, Univ. of Minho,
Portugal
Adjunct Professor, Univ. of Guelph, Canada



Professor at Department of Biology,
University of Minho, Portugal

Distinguished Professor at State Key
Laboratory of Quality Research in
Chinese Medicine, University of
Macau